ECOLOGY

Defensive polyketides produced by an abundant gastropod are candidate keystone molecules in estuarine ecology

Paul Scesa[1], Helen Nguyen[2], Paige Weiss[2], Alejandra P. Rodriguez[2], Matthew Garchow[2], Shannon I. Ohlemacher[3]†, Evangelia Prappas[2], Serena A. Caplins[4], Carole A. Bewley[3], Laine Bohnert[5], Amanda J. Zellmer[5], Eric M. Wood[2], Eric W. Schmidt[1], Patrick J. Krug[2]*

Secondary metabolites often function as antipredator defenses, but when bioactive at low concentrations, their off-target effects on other organisms may be overlooked. Candidate "keystone molecules" are proposed to affect community structure and ecosystem functions, generally originating as defenses of primary producers; the broader effects of animal chemistry remain largely unexplored, however. Here, we characterize five previously unreported polyketides (alderenes A to E) biosynthesized by sea slugs reaching exceptional densities (up to 9000 slugs per square meter) in Northern Hemisphere estuaries. Alderenes comprise only 0.1% of slug wet weight, yet rendered live slugs or dead flesh unpalatable to three co-occurring consumers, making a potential food resource unavailable and redirecting energy flow in critical nursery habitat. Alderenes also displaced infauna from the upper sediment of the mudflat but attracted ovipositing snails. By altering communities, such compounds may have unexpected cascading effects on processes ranging from bioturbation to reproduction of species not obviously connected to the producing organisms, warranting greater attention by ecologists.

INTRODUCTION

For over 50 years, ecological theory has recognized the disproportionate impact of keystone species, taxa that control tipping points between alternative states and have many strong links in interaction networks relative to their abundance (*1*–*4*). Advances in chemical ecology led to the hypothesis that "keystone molecules" may analogously affect food webs and community structure, altering expected patterns of energy flow and species distributions at low relative concentrations (*5*–*10*). Such compounds may mediate diverse ecological processes because chemosensory mechanisms are evolutionarily conserved among taxa, and molecules often persist and propagate through food webs. For instance, the same toxin can deter generalists yet attract specialist feeders that accumulate it for their defense; other life stages or species may then detect or deploy that toxin as a pheromone or alarm cue (*9*). However, keystone molecules are not well integrated into theories of community or ecosystem-scale processes (*7*–*9*).

Food webs based on marine phytoplankton are often affected in complex ways by algal defensive molecules. Compounds like saxitoxin produced by harmful algal blooms become concentrated at higher trophic levels and can be used by resistant species in defense or as chemosensory cues; by altering foraging behavior of predators, such toxins influence community structure and drive large-scale effects associated with red tides (*7*, *10*, *11*). In pelagic systems, dimethyl sulfide (DMS) is produced enzymatically as a breakdown product when phytoplankton are ingested and may directly affect grazing rates and gut physiology of consumers at low trophic levels (*12*). DMS also attracts foraging sea birds at great distances to high-productivity patches where fish and crustacean consumers gather (*13*, *14*), and DMS signaling promotes energy transfer from marine to terrestrial systems when seabirds excrete wastes on island roosts (*7*, *15*).

Pyrrolizidine alkaloids (PAs) from plants play similarly diverse roles in terrestrial ecosystems, altering the composition of the rhizosphere. PAs suppress hyphal growth in endophytic fungi associated with species lacking PAs, but not mutualistic fungi of PA-producing species (*16*). These compounds also act as oviposition cues for specialized arctiid moths, which sequester PAs as antipredator defenses and as mate attractants (*9*, *17*, *18*). Microbial metabolites may also regulate soil nutrient cycling and plant primary production, but there is a lack of theory synthesizing the impacts of keystone molecules across marine and terrestrial systems (*19*).

Notably, classic keystone species were recognized through top-down effects, whereas most proposed keystone molecules influence communities via bottom-up effects. However, many primary consumers are chemically rich and rely on secondary metabolites for defense and signaling, including insects (*20*), gastropods (*21*), and filter-feeding invertebrates (*22*). Defensive compounds in abundant consumers may affect food webs by limiting the energy from primary production reaching higher trophic levels. Keystone molecule status may be warranted when a feeding deterrent further links a consumer to other community members in interaction networks through unexpected responses. For instance, many bioactive compounds show both antifeedant and antimicrobial activity, so they could deter predators while changing the microbiome of surrounding sediments or surfaces (*22*). The same secondary metabolite could alter community structure by differentially attracting or repelling species that would not otherwise interact with the producing organism or disrupting ecological processes regulated by chemical signaling like spawning or recruitment (*23*).

[1]Department of Medicinal Chemistry, University of Utah, Salt Lake City, UT 84112, USA. [2]Department of Biological Sciences, California State University, Los Angeles, CA 90032, USA. [3]Laboratory of Bioorganic Chemistry, National Institute of Diabetes and Digestive and Kidney Diseases, National Institutes of Health, Bethesda, MD 20892, USA. [4]Department of Population Biology, University of California at Davis, Davis, CA 95616, USA. [5]Department of Biology, Occidental College, 1600 Campus Rd., Los Angeles, CA 90041, USA.
*Corresponding author. Email: pkrug@calstatela.edu
†Present address: Gennao Bio, Princeton, NJ 08534, USA.

Sea slugs (marine heterobranch gastropods) generally lack a protective shell and use alternative defenses such as sequestering diet-derived compounds (*21*) and cnidarian nematocysts (*24*), or de novo biosynthesis of deterrents (*21*). Ecological impacts of sea slugs have primarily been recognized in disturbed systems: the loss of pteropods due to ocean acidification (*25*), alteration of infaunal communities by invasive predators (*26*), or control of introduced macroalgae by herbivores (*27*). However, bioactive metabolites of sea slugs may play a keystone role by protecting impactful consumers that would otherwise be abundant prey items while exerting unrecognized effects on the surrounding community (*28*). Here, we show that sea slugs in the genus *Alderia* are exceptionally abundant grazers in boreal to warm-temperate estuaries throughout the Northern Hemisphere, but a chemical defense protects this potential food resource from predation, shunting substantial energy away from higher trophic levels. The compounds are released in slug pedal mucus and potentially in concentrated pulses during mass die-off events. Field experiments reveal that slug compounds trigger rapid changes in the abundance of nearby infauna; thus, defensive metabolites have unexpected effects on food webs and community structure, with potential ecosystem-level implications.

RESULTS

Boom-and-bust population dynamics of *Alderia*, an abundant estuarine grazer

The yellow-green (heterokont) alga *Vaucheria* is a dominant primary producer in the high intertidal zone of mudflats, forming mossy mats that stabilize sediment. In Northern Hemisphere estuaries, amphibious sea slugs in the genus *Alderia* specialize on *Vaucheria*, surviving in nearly fresh water to fully marine conditions and living out of water for extended periods (*29*–*31*). European slugs are *Alderia modesta* (Lovén, 1844), while a divergent but externally cryptic species, *A.* cf. *modesta*, is widely distributed from San Francisco Bay, USA throughout the North Pacific and western North Atlantic (*32*–*34*). A distinctive congener, *Alderia willowi* [Krug, Ellingson, Burton, and Valdés, (*35*, *36*)], is found in California, USA.

Alderia spp. are small, 2- to 12-mg wet weight (*37*, *38*), but often extraordinarily abundant (table S1). Pooling data across all three species, mean slug density throughout the year increased with latitude (Fig. 1A, and results of a linear regression: $P < 0.0001$). Most populations averaged from 100 to 800 slugs/m^2, but the highest latitude population of *A. modesta* had a mean of ~5000 slugs/m^2 (*31*). Peak density for a year also increased with latitude (Fig. 1B, and results of a linear regression: $P < 0.0001$). Most populations peaked at 1000 to 5000 slugs/m^2, but at the highest latitude, maximum density was a remarkable ~9000 slugs/m^2. Even low-latitude populations of *A. willowi* achieved high mean (>150 slugs/m^2) and peak densities (>1000 slugs/m^2).

Population dynamics of both *A.* cf. *modesta* and *A. willowi* were tracked for several years in Mill Valley, San Francisco Bay (Fig. 1, C and D) (*38*). Each species had one peak in annual abundance following a major recruitment event. Densities of *A.* cf. *modesta* peaked in February and March when most individuals were juveniles (<2-mg wet weight) (Fig. 1C); although mean densities for Mill Valley ranged from 650 to 1150 slugs/m^2 ($N = 3$ years), peak local densities exceeded 11,000 slugs/m^2. However, 1 month later, densities declined by 72% (±8% SE; $N = 3$ years). Maximum annual mud temperatures occurred each in April and May, coinciding with observed mass die-off events. In April 2008, maximum mud temperature during low tides was 41.1°C on a transect where 82.8% (±9.4% SE; $N = 4$ quadrats) of slugs were discolored and dying in the field; mortality was confirmed by microscopic examination over several hours after collection. In April 2009, 36.5% (±14.9% SE; $N = 4$) of slugs from the same transect were dead in the field on a day when maximum mud temperature was 34.4°C, as were a smaller proportion of slugs from two nearby transects (Fig. 1E). Such temperatures exceed the tolerance of *Alderia* spp. (*39*). Surviving slugs grew larger but rarer through summer; although the population declined by >99%, *A.* cf. *modesta* was present year-round.

In contrast, *A. willowi* was absent from San Francisco Bay from March to August, recruiting in late summer (Fig. 1D). Abundance peaked in October and November; maximum density was 1393 ± 387 slugs/m^2 in 2008. *A. willowi* produces both dispersive larvae and also nondispersive offspring that recruit locally (*36*, *38*); cohorts therefore overlap, and size and density were uncorrelated (Fig. 1D). Although mass die-offs were not directly observed, seasonal mortality was equally marked for *A. willowi*, with abundance falling by 51 ± 5% (±SE; $N = 2$ years) within 1 to 2 months of peak density, and >99% by January and February for each annual cohort. Although lacking detailed surveys, similar population cycles were inferred for *Alderia* spp. at more northern latitudes (*29*–*33*, *37*).

Assuming brackish emergent tidal marsh represents suitable habitat for *Alderia*, mean fall biomass was estimated as 170 kg for Mill Valley (Fig. 1E) and >15,000 kg for all mudflats in San Francisco Bay; mean estimates for spring were 860 kg in Mill Valley and >75,000 kg for San Francisco Bay. At peak densities, estimated biomass of *A. willowi* was >1100 kg for Mill Valley and >100,000 kg for San Francisco Bay, and for *A.* cf. *modesta*, >2300 kg in Mill Valley and >200,000 kg in San Francisco Bay. If even a fraction of tidal marsh is colonized by slugs, *Alderia* populations may thus represent a large potential food source for invertebrate predators, juvenile fish, and migratory waterfowl or resident shorebirds (*33*).

Polyketides and their biosynthesis in *Alderia*

Slugs on the mudflat lack obvious defenses, but if slugs are chemically defended, primary production from *Vaucheria* may be shunted away from higher trophic levels. As both consumers and potential prey, the role of *Alderia* in estuarine food webs thus remains an open question with implications for resource distribution in sensitive nursery habitat across the Northern Hemisphere (*39*–*41*). Boom-and-bust population dynamics also suggest that defensive chemistry might be released into the environment during episodic mass die-offs with potentially widespread community effects.

Alderia have a pungent scent, but no prior study analyzed their secondary metabolite profile. Phylogenetic evidence suggested that *Alderia* might biosynthesize polyketides (PKs), secondary metabolites with a range of biological activities. Superorder Sacoglossa contains superfamilies Plakobranchoidea—comprising chloroplast-retaining, photosynthetic species—and Limapontioidea—comprising largely nonphotosynthetic taxa (including *Alderia*) with dorsal appendages termed cerata that may autotomize (*42*). We recently characterized a previously unrecognized branch of PK-synthesizing enzymes [animal fatty acid-like polyketide synthases (AFPKs)] in protostome bilaterians (*43*–*45*). In highly photosynthetic species in Plakobranchoidea, the enzymes EcPKS1 and EcPKS2 produce unsaturated, medium- and long-chain pyrones using methylmalonyl–coenzyme A as a substrate, otherwise unknown in animal lipid metabolism. The

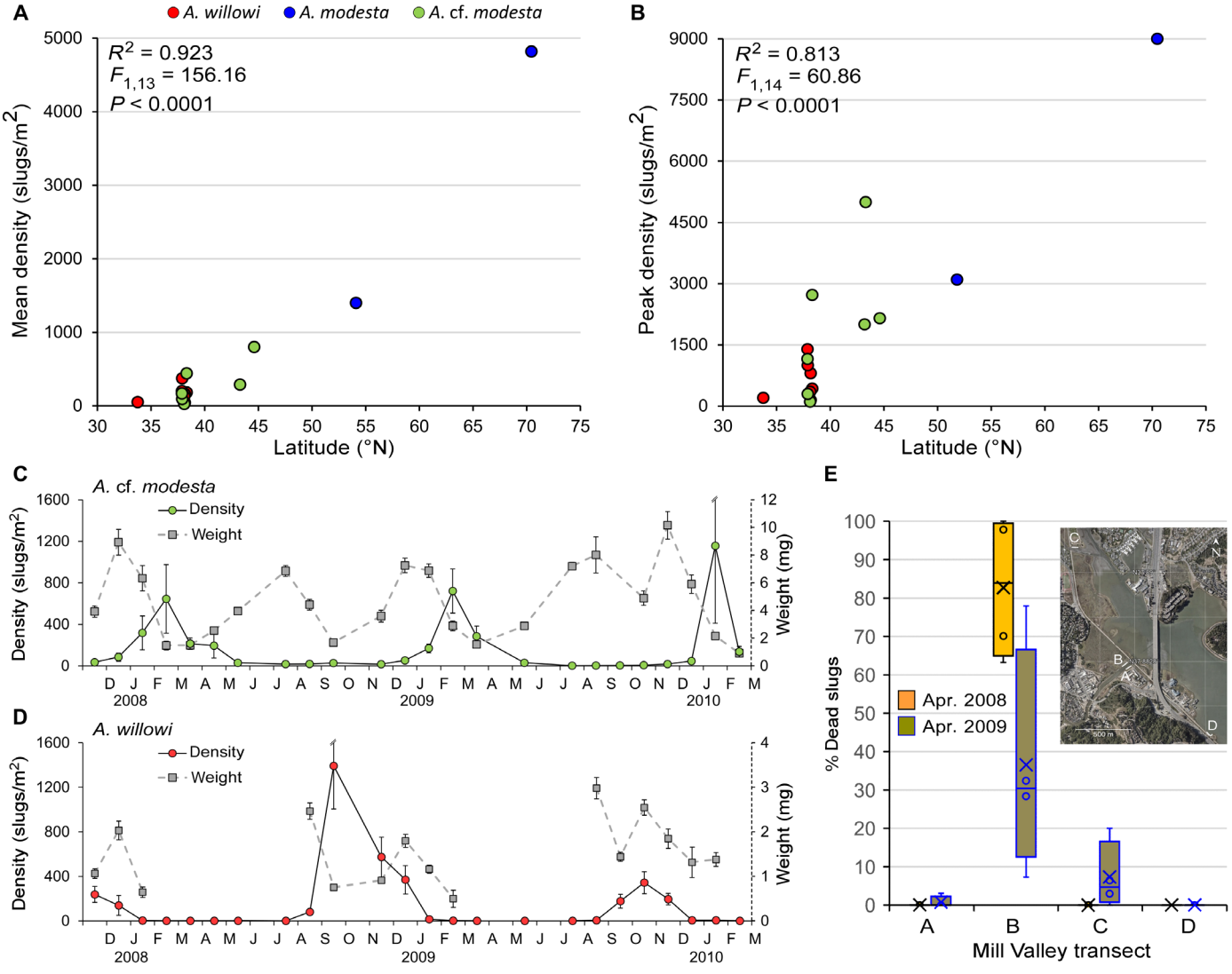

Fig. 1. Density and population dynamics of *Alderia* spp. (**A** and **B**) Exceptional mean (A) and peak (B) population densities scale with latitude in *A. modesta* (blue), *A.* cf. *modesta* (green), and *A. willowi* (red). (**C** and **D**) Seasonal abundance and growth of *Alderia* spp. cohorts in San Francisco Bay from 2008 to 2010. Mean number (± SE) of slugs/m^2 plotted for *A.* cf. *modesta* (green circles) and *A. willowi* (red circles), with wet weight (gray squares, dashed lines); $N = 16$ quadrats per survey. (**E**) Mass die-offs in *A.* cf. *modesta* coinciding with peak annual mud temperatures in April of 2008 and 2009. Inset, map of Mill Valley, San Francisco Bay, showing four permanent transects.

longer unsaturated pyrones may facilitate animal photosynthesis due to their antioxidant or photoprotective properties, usually forming additional cyclic motifs (*43*). In contrast, cerata-bearing slugs expressed different lineages of AFPKs (*44*), and all species studied to date contained short-chain, monocyclic PKs of unknown function. AFPKs are prevalent in shell-less gastropods that otherwise lack strong diet-derived defenses, suggesting a potential antipredator function (*45*). However, large fish and crab species consumed *Alderia* over a 3-day trial in one prior study (*46*).

Inspired by their odor and abundance, we chemically characterized both *Alderia* spp. from California. Liquid chromatography–mass spectrometry (LC-MS) analysis of acetone extracts of individual *A.* cf. *modesta* and *A. willowi* revealed peaks with fragmentation patterns and molecular masses consistent with sacoglossan PKs (Fig. 2A and table S2). Individually analyzed *A.* cf. *modesta* ($N = 7$) contained at least five PKs in proportions that varied only slightly among individuals (fig. S1). Two of the compounds (**1** and **5**) were also present in *A. willowi*, again in proportions that varied minimally among individual slugs ($N = 7$).

Acetone extraction of ~200 whole *A. modesta* specimens, followed by dichloromethane extraction and LC-MS, revealed the presence of at least five PK metabolites, each with five degrees of unsaturation and varying degrees of methylenation. Reversed-phase flash chromatography on C_{18} followed by semi-preparative high-performance LC (HPLC) on a phenylhexyl column led to the purification of five new cyercene-class metabolites, alderenes A to E (**1** to **5**) (Fig. 2B). Structures were elucidated by one-dimensional (1D) and 2D nuclear magnetic resonance (NMR) experiments [heteronuclear multiple-quantum coherence, heteronuclear multiple-bond correlation (HMBC), and correlation spectroscopy (COSY)] plus tandem MS. All alderenes exhibited strong ultraviolet (UV) absorptions with λ_{max} values between 232 and 235 nm, and infrared (IR) bands around 1712 cm^{-1} typical of α-pyrones. Compared to

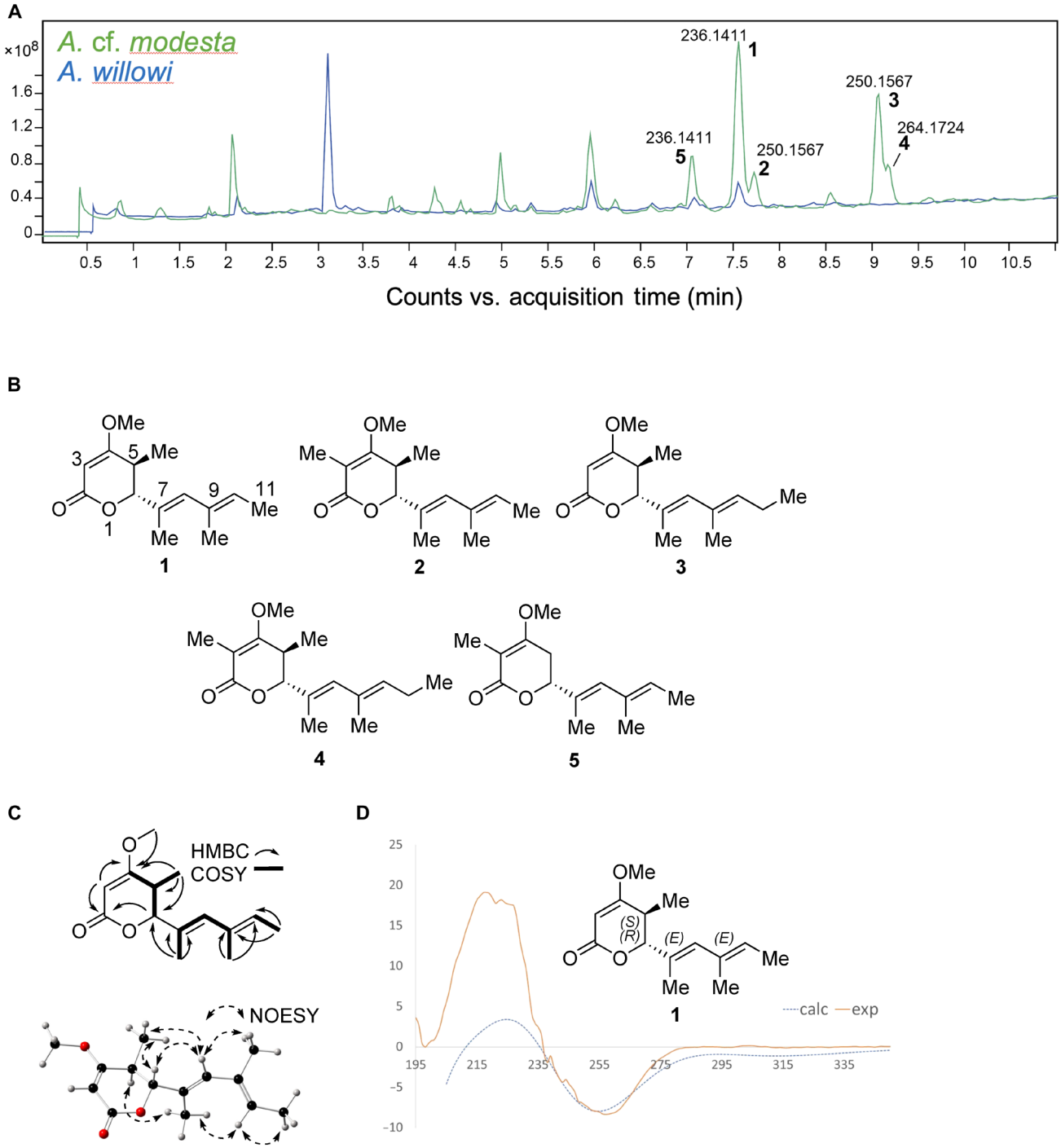

Fig. 2. Alderenes A to E, new PKs isolated and characterized from *Alderia*. (**A**) Overlaid LC-MS traces of acetone extracts of an individual *A.* cf. *modesta* (green) and *A. willowi* (blue), showing the molecular masses of five PKs, two from both species (**1** and **5**) and the remainder from *A.* cf. *modesta*. (**B**) Structures for alderenes A to E (**1** to **5**). (**C**) Structure elucidation and relative configuration of alderene A (**1**) determined by 2D NMR experiments. (**D**) Comparison of experimental versus calculated ECD spectra confirmed the structure and absolute configuration of **1** as diagrammed.

polypropionate pyrones reported from related molluscs (*47*–*51*), these data indicated that the *Alderia* metabolites represented a class of dihydro-α-pyrones with a reduced head group, unprecedented from sacoglossans. Metabolites differed from one another on the basis of various degrees of methylenation, likely reflecting the incorporation of malonyl versus methylmalonyl precursors during PK chain extension.

Electrospray ionization (ESI)–MS spectra of alderene A (**1**) suggested the molecular formula $C_{14}H_{20}O_3$ with an observed ion at mass/charge ratio (*m*/*z*) 259.1310 $[M + Na]^+$ (calc. *m*/*z* 259.1305), which was also supported by the overall ^{13}C NMR data (Table 1). An intense IR band at 1711 cm^{-1} together with a ^{13}C NMR signal at δ_C 163.9 indicated the presence of a conjugated ester with a UV

maximum at 232 nm. The γ-pyrone ring of **1** was characterized by ^{13}C NMR resonances of δ_C 167.3 (C-2), 89.7 (C-3), 175.8 (C-4), 34.3 (C-5), and 88.8 (C-6), as well as by four ^{1}H NMR signals at δ_H 5.11 (H-3), 3.74 (Me-O), 2.80 (H-5), 4.35 (H-6), and 1.04 (Me-5) (Table 1, Fig. 2B, and Supplementary NMR data). Correlations in the 2D COSY spectrum between H-5 and H-6 supported the structure of the dihydro-α-pyrone; this structure was confirmed by correlations in the 2D HMBC, with the position of the enol ether indicated by the cross-peak between the Me-O proton resonance and the C-4 resonance. The presence of the lactone was confirmed by cross peaks between H-6 and C-2 resonances (Fig. 2C and Supplementary NMR data). The ^{1}H NMR spectrum of **1** also showed two downfield resonances, δ_H 5.91 (H-8) and 5.43 (H-10), that were attributed to the protons of two side-chain double bonds, as well as three olefinic methyl resonances, δ_H 1.80 (Me-7), 1.74 (Me-9), and 1.68 (C-11) (Table 1). The presence of four additional olefinic resonances in the ^{13}C NMR at δ_C 129.2 (C-7), 135.8 (C-8), 132.5 (C-9), and 126.1 (C-10) further supported the presence of this side chain. The connection of the pyrone ring with the unsaturated side chain and the respective position of each methyl group was unambiguously assigned by an array of cross peaks in the HMBC spectrum (Fig. 2C).

The relative configuration of **1** was determined by NMR data analysis, using nuclear Overhauser effect and *J* coupling relationships as well as chemical shift arguments. A lack of 2D nuclear Overhauser effect spectroscopy (NOESY) correlations between H-8 and the Me-7 $^{1}H_3$ resonances, as well as between H-10 and the Me-9 $^{1}H_3$

Table 1. Chemical shifts for alderenes A to E (1 to 5) in $CDCl_3$, based on ^{13}C NMR and ^{1}H NMR experiments.

^{13}C NMR experiment					
Position	δ_C				
	1*	2†	3*	4*	5†
2	167.3 (C)	167.8 (C)	167.2 (C)	168.0 (C)	168.9 (C)
3	89.7 (CH)	105.3 (C)	89.7 (CH)	105.2 (C)	103.3 (C)
4	175.8 (C)	168.6 (C)	175.8 (C)	168.7 (C)	165.4 (C)
5	34.3 (CH)	31.7 (CH)	34.3 (CH)	31.9 (CH)	27.7 (CH_2)
6	88.8 (CH)	85.8 (CH)	88.8 (CH)	85.9 (CH)	80.4 (CH)
7	129.2 (C)	129.9 (C)	131.0 (C)	131.0 (C)	130.6 (C)
8	135.8 (CH)	133.3 (CH)	135.9 (CH)	133.5 (CH)	132.7 (CH)
9	132.5 (C)	132.5 (C)	133.8 (C)	133.4 (C)	132.2 (C)
10	126.1 (CH)	125.7 (CH)	129.4 (CH)	130.2 (CH)	125.8 (CH)
11	13.8 (CH_3)	13.5 (CH_3)	21.6 (CH_2)	21.6 (CH_2)	13.5 (CH_3)
Me-3	-	9.5 (CH_3)	-	9.7 (CH_3)	8.6 (CH_3)
Me-5	12.0 (CH_3)	16.0 (CH_3)	12.0 (CH_3)	16.3 (CH_3)	-
Me-7	13.0 (CH_3)	14.5 (CH_3)	13.0 (CH_3)	14.6 (CH_3)	13.4 (CH_3)
Me-9	16.5 (CH_3)	16.5 (CH_3)	16.6 (CH_3)	16.7 (CH_3)	16.1 (CH_3)
Me-11	-	-	14.1 (CH_3)	14.2 (CH_3)	-
Me-O	56.4 (CH_3)	57.0 (CH_3)	56.4 (CH_3)	57.1 (CH_3)	55.2 (CH_3)
^{1}H NMR experiment					
Position	δ_H				
	1‡	2§	3‡	4§	5§
3	5.12 (s)	-	5.12 (s)	-	
5	2.80 (dq, 10.8, 7.0)	2.85 (p, 7.0)	2.79 (dq, 10.8, 7.0)	2.86 (p, 7.0)	2.71 (dq, 17.0, 12.3, 2.3)
	-	-	-	-	2.52 (ddd, 17.0, 4.1, 1.2)
6	4.35 (d, 10.8)	4.44 (d, 5.5)	4.34 (d, 10.8)	4.45 (d, 5.5)	4.69 (dd, 12.3, 3.5)
8	5.91 (s)	5.82 (s)	5.91 (s)	5.82 (s)	5.98 (s)
10	5.43 (br q, 5.9)	5.38 (br q, 5.9)	5.35 (t, 5.9)	5.28 (t, 5.9)	5.45 (br q, 7.0)
11	1.68 (d, 6.4)	1.67 (d, 6.4)	2.10 (p, 7.0)	2.08 (p, 7.0)	1.69 (d, 7.0)
Me-3	-	1.70 (s)	-	1.81 (s)	1.79 (s)
Me-5	1.04 (d, 7.0)	1.22 (d, 7.0)	1.03 (d, 7.0)	1.22 (d, 7.0)	-
Me-7	1.80 (d, 1.2)	1.81 (s)	1.81 (s)	1.76 (s)	1.85 (d, 1.2)
Me-9	1.74 (s)	1.76 (s)	1.73 (s)	1.69 (s)	1.74 (s)
Me-11	-	-	0.99 (t, 7.0)	0.98 (t, 7.0)	-
Me-O	3.74 (s)	3.78 (s)	3.74 (s)	3.79 (s)	3.79 (s)

*Measured at 125 MHz. †Measured by inverse detection. ‡Measured at 500 MHz. §Measured at 600 MHz.

resonances, suggested an *E*,*E*-geometry of the side chain; this configuration was further supported by the relatively low ^{13}C chemical shifts for Me-7 (δ_C 13.0) and Me-9 (δ_C 16.5), which are typical of *E*-configured polypropionates (*46*, *48*). Comparing molecular models for each diastereomer in its various conformational states, assisted by density functional theory (DFT) optimization and free energy calculations, facilitated analysis of NOESY data. It was determined that the *E*,*E*-diene preferred two near *S*-cis conformations twisted out of plane by ±45° in either direction, likely due to substantial $A^{1,3}$ strain between Me-7 and Me-9. For the pyrone ring in a trans configuration, two half chair conformations were determined, with H-5 and H-6 adopting a preferred axial orientation. Another conformational state with H-5 and H-6 equatorial likely accounts for the 10-Hz coupling between these protons. This overall structure was confirmed using NOESY correlations (Fig. 2C). NOESY cross peaks between H-5 and Me-7 and between Me-7 and H-10 indicated that the planes of the diene chain and pyrone ring were nearly orthogonal, with these protons oriented toward the α-face of the ring. NOESY correlations between Me-5 and H-6 indicated their *cis* orientation on the ring, and correlations from H-8 to Me-5, H-6 and Me-9 demonstrated that these protons were all oriented toward the β-face of the pyrone ring. Overall, these data indicated that **1** had the trans-pyrone ring with two *E*-double bonds. To determine the absolute configuration, four conformers of this diastereomer were Boltzmann weighted and the electronic circular dichroism (ECD) spectra computed by time-dependent DFT (TD-DFT). The experimental ECD spectrum was consistent with the predicted spectrum for **1** (Fig. 2D), allowing determination of the 5*S*,6*R*-absolute configuration.

The structures of **2** to **5** were determined primarily by comparison of NMR data to that of **1** (Table 1). Alderenes **1** to **5** all showed similar IR and UV spectra, indicating pyrone and diene functionalities. Different methylation patterns were consistent with the NMR spectroscopic dissimilarities between compounds. Alderenes **2** and **4** had an additional olefinic methyl resonance and an increased chemical shift at C-3, indicating methylation at this site. Alderenes **3** and **4** lacked the Me-11 olefinic methyl doublet, showing instead an aliphatic methyl triplet and additional allylic methylene. Furthermore, **3** and **4** showed an olefinic methine triplet at C-10, indicating that these metabolites were C-11 homologs of **1**. These proposed structural variations were consistent with high-resolution MS and 2D NMR data (fig. S2 and Supplementary NMR data). Alderenes **1** to **4** showed optical rotations of the same sign, and **1** and **3** showed very similar ECD spectra. Hence, **1** to **4** were determined to be of the same absolute configuration on the basis of these properties, while **5** is likely of the same absolute configuration on biogenetic grounds.

Major alderenes are secreted in the pedal mucus of crawling slugs. LC-MS analysis of *Vaucheria* patches on which slugs had recently crawled detected alderenes **1** and **5**, whereas analysis of egg masses did not detect any PKs (fig. S3). In a standard bioassay for antimicrobial activity, alderene A (**1**) inhibited growth of *Staphylococcus aureus* at 25 μg/ml but not *Escherichia coli* or *Acinetobacter baumannii*.

We identified AFPKs in the transcriptome of *A*. cf. *modesta* (*AmPKS1* and *AmPKS2*) that grouped with *EcPKS1* and *EcPKS2* from *E. chlorotica* in the sacoglossan-specific mo-clade 1 (Fig. 3). AmPKS enzymes belong to a subgroup predicted to biosynthesize short-chain pyrones (*44*). Thus, the sequenced genes expressed by *A*. cf. *modesta* are consistent with the structures of the alderenes. Factors leading to the unprecedented reduced dihydro-pyrone ring have yet to be elucidated. Expression of *AmPKS1* was three to five times lower than that of the *FAS1* and *FAS2* genes, normalized to glyceraldehyde-3-phosphate dehydrogenase, whereas expression of *AmPKS2* was comparable to *FAS2* but still less than half that of *FAS1* (Fig. 3, inset).

PKs deter co-occurring predators

We hypothesized that in *Alderia*, PKs primarily function as an adaptation to deter benthic predators likely to encounter small slugs. Antifeedant assays were performed using three size-appropriate, co-occurring mudflat predators: the arrow goby fish *Clevelandia ios*, the polychaete worm *Neanthes arenaceodentata*, and the lined shore crab *Pachygrapsus crassipes*. All worms made repeated predation attempts on live *A*. cf. *modesta*, attacking slugs 2.3 times ±0.4 SE more often than squid mantle (positive control), which was consumed after one bite (sign test, $P = 0.002$). Every worm ($N = 20$) ultimately rejected the slug but consumed squid controls (Table 2; Fisher's exact test, $P = 7 \times 10^{-12}$); worms often demonstrated a stress response such as shaking the head, repeatedly everting the proboscis, or backing away from slugs (movie S1). Similarly, crabs ($N = 9$) rejected all live *A*. cf. *modesta* but ate squid controls (Table 2; Fisher's exact test, $P = 2 \times 10^{-5}$). Most crabs passed the slug over their mouthparts and then dropped the slug. Two crabs attempted to feed on *A*. cf. *modesta* but spent most of the trial pulling mucus strands from their mouth, ultimately dropping the slug (movie S2). Controls were consumed in a significantly shorter time, 25.1 s ± 3.0 SE (fig. S4A). All slugs survived for 7 days after crab predation attempts. Fish ($N = 10$) attacked live *A*. cf. *modesta* 2.8 times ± 0.3 SE (range, one to four attacks) but made just one attempt per control (sign test, $P = 0.002$), rejecting all live slugs while consuming squid controls (Table 2; Fisher's exact test, $P = 5 \times 10^{-6}$). Fish spent significantly longer mouthing an *A*. cf. *modesta* (29.4 s ± 4.3 SE) compared to controls (8.1 s ± 0.6 SE) before finally expelling the slug (movie S3).

Responses to live *A. willowi* were comparable. Worms rejected all live slugs ($N = 10$) (Table 2; $P = 5 \times 10^{-6}$) after making about twice as many feeding attempts compared to controls (sign test, $P = 0.002$). Crabs ($N = 9$) ate no live *A. willowi* (Table 2; $P = 2 \times 10^{-5}$); four attempted to feed for the whole trial but consumed only 1 mm ± 0.2 SE of a slug's body (5-mm mean length). Crabs spent most of the trial removing mucus from their mouth, whereas controls were consumed in only 11.5 s ± 1.6 SE (fig. S4B). All slugs survived 7 days after attempted crab predation. Fish ($N = 10$) consumed no live *A. willowi* but ate all controls (Table 2; $P = 5 \times 10^{-6}$), attacking slugs 4.1 times ± 0.4 SE (range, one to six attacks) versus one attempt per control (sign test, $P = 0.002$). Fish spent 24.4 s ± 3.8 SE mouthing *A. willowi* versus 7.1 s ± 1.0 SE to consume controls.

To determine whether active secretion of mucus was an essential component of slug defense, we tested the palatability of dead slugs that had been flash-frozen and then thawed immediately before assays. All worms, crabs, and fish rejected every dead *A*. cf. *modesta* offered but ate all controls (Table 2); behavioral reactions of predators were comparable to feeding attempts with live slugs. Fish spent 25.7 s ± 3.2 SE mouthing slug bodies before rejection, versus 7.5 s ± 0.7 SE to consume controls. All predators similarly rejected every dead *A. willowi* (Table 2), with fish again spending about three times longer mouthing slug bodies before rejection (21.8 s ± 3.1 SE) versus time to consume controls (6.8 s ± 0.6 SE). Thus, mucus secretion was not required for slug tissue to repel hungry mudflat consumers.

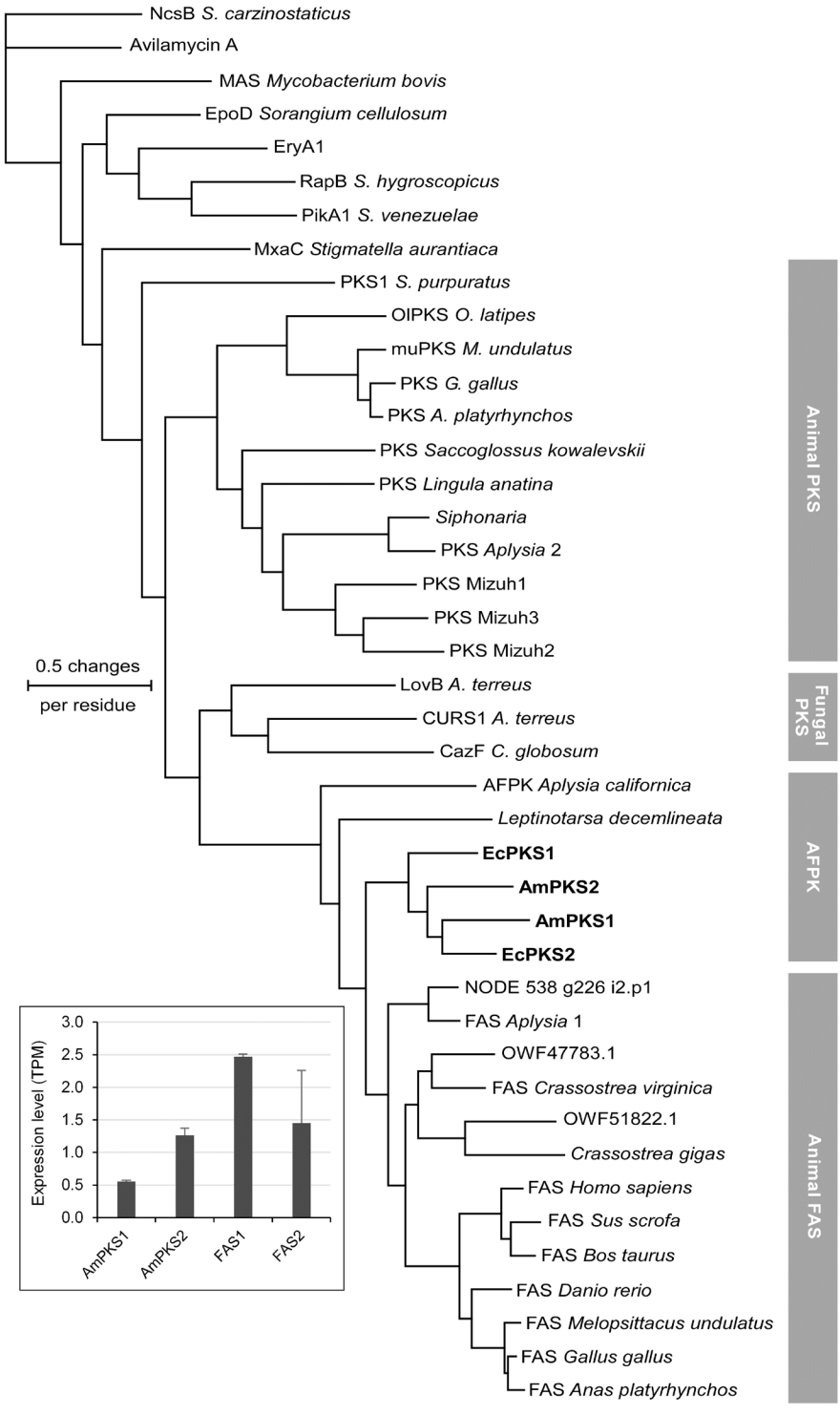

Fig. 3. Evolutionary relationships of animal polyketide synthase (PKS), animal fatty acid-like polyketide synthase (AFPK), and animal fatty acid synthase (FAS) protein sequences, based on maximum-likelihood analysis. Boldfaced tip labels show a clade comprising AFPK enzymes from photosynthetic sacoglossans (EcPKS1 and EcPKS2) and orthologs from *A.* cf. *modesta* (AmPKS1 and AmPKS2). **Inset**, expression of FAS and AFPK genes from *A.* cf. *modesta* relative to glyceraldehyde-3-phosphate dehydrogenase, estimated as transcripts per million (TPM).

Table 2. Predator response to potential prey items, compared to an identical number of positive control items that were 100% consumed in every trial.

Treatment	Slug species	Predator	# Prey items eaten	Total # prey offered	*P* value*
Live slug	*A. willowi*	Worm	0	10	5×10^{-6}
		Crab	0	9	2×10^{-5}
		Fish	0	10	5×10^{-6}
	A. cf. *modesta*	Worm	0	20	7×10^{-12}
		Crab	0	9	2×10^{-5}
		Fish	0	10	5×10^{-6}
Dead slug, intact	*A. willowi*	Worm	0	10	5×10^{-6}
		Crab	0	10	5×10^{-6}
		Fish	0	10	5×10^{-6}
	A. cf. *modesta*	Worm	0	10	5×10^{-6}
		Crab	0	10	5×10^{-6}
		Fish	0	10	5×10^{-6}
Dead slug, solvent-extracted	*A. willowi*	Worm	10	10	n.s.
		Crab	10	10	n.s.
		Fish	10	10	n.s.
	A. cf. *modesta*	Worm	10	10	n.s.
		Crab	10	10	n.s.
		Fish	10	10	n.s.
Egg mass, intact	*A. willowi*	Worm	10	10	n.s.
		Crab	10	10	n.s.
		Fish	5	10	3×10^{-2}
Egg mass, halved	*A. willowi*	Fish	10	10	n.s.
Pellet: organic layer, slug extract	*A. willowi*	Crab	0	10	5×10^{-6}
		Fish	0	10	5×10^{-6}
	A. cf. *modesta*	Crab	0	10	5×10^{-6}
		Fish	0	10	5×10^{-6}
Pellet: PK-enriched	*A. willowi*	Fish	0	10	5×10^{-6}

**P* value denotes significant difference based on Fisher's exact test between proportion of prey items versus controls (comparably processed squid mantle) consumed in a trial; n.s., not significant.

We next tested whether removing nonpolar secondary metabolites would restore the palatability of slug tissue by offering predators intact slug bodies that had been extracted twice with acetone to remove small organic compounds. All worms, crabs, and fish consumed 100% of extracted *A.* cf. *modesta* and *A. willowi* (Table 2). Worms (fig. S5, A and D) and fish (fig. S5, C and F) consumed acetone-extracted slugs of both *Alderia* spp. in the same time as extracted squid controls; crabs took longer to consume extracted *A.* cf. *modesta* (fig. S5B; independent *t* test, $t_{16} = 3.5$, $P < 3 \times 10^{-3}$) and extracted *A. willowi* (fig. S5E; independent *t* test, $t_{16} = 3.5$, $P < 3 \times 10^{-3}$) than squid controls.

All worms and crabs consumed intact egg masses of *A. willowi* as readily as squid mantle controls (Table 2), displaying no adverse reaction to the egg mases during feeding. Half of the tested fish ($N = 10$) rejected *A. willowi* egg masses but ate controls—a significant effect (Table 2; results of a Fisher's exact test: $P = 0.03$). Fish displayed no adverse reactions to egg masses, but some appeared unable to handle intact egg masses with their mouths. In contrast, all fish consumed egg masses cut in half, exposing the gelatinous inner egg strand (Table 2). The results suggested that the weak deterrent effect on fish was due to the physical protection offered by the tough outer covering of egg masses and not to a chemical defense, while worms and crabs were more easily able to penetrate the outer coat to feed on the undefended eggs.

To confirm that the deterrent effects of slug tissue were due to alderenes, we tested organic extracts of *Alderia* incorporated into squid pellets. Acetone extracts were concentrated and then partitioned between water and ethyl acetate, yielding an organic layer enriched in PKs and nonpolar metabolites (lipids, chlorophyl from dietary algae).

The organic layer was concentrated and tested at 100% of the natural concentration per wet weight for both *Alderia* spp. Crabs rejected all pellets incorporating *A. cf. modesta* extract but ate all control pellets made with an equal volume of carrier solvent (Table 2; Fisher's exact test: $P = 5 \times 10^{-6}$). Crabs passed extract-containing pellets over mouthparts using chelae before discarding the pellets (2.7 s ± 1.0 SE), spending longer to consume control pellets (7.4 s ± 1.0 SE, fig. S6A; independent *t* test, $t_{18} = 3.3$, $P < 4 \times 10^{-3}$). Fish ultimately rejected all extract-containing pellets while consuming all control pellets (Table 2; Fisher's exact test, $P = 5 \times 10^{-6}$). Fish made more attempts on treated pellets (3.0 ± 0.5 SE; range = 1 to 5) before rejection, while controls were attacked once and consumed (fig. S6B; results of a sign test, $P = 0.002$). After tasting extract pellets, some fish reacted by rapidly opening and closing their mouth while fanning gills and everting pharyngeal jaws. Similarly, the organic layer from extract of *A. willowi* deterred all crabs compared to controls (Table 2) and hastened rejection of pellets versus time to consume controls (fig. S6C; independent *t* test, $t_{18} = 5.2$, $P < 10^{-4}$). Fish also rejected all pellets containing extract of *A. willowi* at 100% of natural concentration, with most quickly abandoning treated pellets, whereas longer times were spent fully consuming controls (fig. S6D).

For bioassay-guided fractionation, we further partitioned the organic layer between hexane, yielding a fraction primarily of fats and sterols, and methanol, yielding a fraction that was ~95% alderenes by NMR spectroscopy (fig. S7). Pellets containing the PK-enriched fraction from *A. willowi* (100% of concentration in tissue by wet weight) were rejected by fish, while controls were all consumed (Fisher's exact test, $P = 5 \times 10^{-6}$), as were all pellets incorporating the hexane fraction. We therefore compared the feeding response to pure alderenes **1** and **5** versus crude extract of *A. willowi* and solvent-only control pellets. Because of limited quantities of pure metabolites, assays testing either compound **1** or **5** used the smallest pellets that could be made, which predators were sometimes able to ingest after repeated attempts broke a pellet into pieces (whereas larger pellets were always rejected). We therefore included small pellets with crude extract as a positive control for aversion or deterrence, for comparison.

For crabs, pure compounds or crude extract did not reduce initial prey-sampling time compared to controls (fig. S8) but induced aversive reactions after feeding began. The same behaviors were induced by pellets incorporating pure alderenes and crude extract, but not controls: Crabs bubbled at the mouth, wiped mouthparts with appendages, or rubbed mouthparts against the substrate. Reactions to **5** lasted roughly twice as long as to **1** at both 25 and 50% of natural concentrations in slugs (fig. S8, B and D; $P < 0.01$, Mann-Whitney test) but three times longer for crude extract than for **5**. Both **1** and **5** inhibited crab feeding responses, halving the number of cheliped movements from pellets to mouth at 25% (fig. S9A), 50% (fig. S9C), and 100% (fig. S9E) of the natural concentration per slug wet weight as effectively as crude extract. All treatments differed significantly from controls except for 25% of **1**; pure alderenes were thus sufficient to inhibit feeding responses. All concentrations of **1** and **5** also increased the number of times crabs pulled material from their mouths after feeding by 10- to 20-fold, a response induced by live slugs and crude extract but not controls (fig. S9, B, D, and F; paired sign test, $P < 0.005$). All concentrations of **5** and crude extract also significantly increased the proportion of crabs that rubbed or pressed mouthparts against the substrate after ingesting treated pellets, behavior not induced by **1** or controls (fig. S10).

Fish regurgitated two to three times more often when fed pellets incorporating **1** (paired sign test, $P < 0.005$) or extract ($P < 0.01$) at 50% of the natural concentration, significantly more than controls (fig. S11B); **5** had a borderline effect ($P = 0.07$). Only crude extract induced regurgitation at 25% of the natural concentration (fig. S11). Neither alderene nor crude extract reduced prey handling time before initial feeding attempts by fish (fig. S12, A and C; $P > 0.1$). However, both alderenes increased the time fish spent mouthing, regurgitating, and trying to ingest a pellet after the initial bite at 25% (fig. S12B; paired sign test, $P < 0.05$), and for **1** at 50% (fig. S12D; paired sign test, $P < 0.01$) of the native concentration in slugs. Response to alderenes and crude extract was comparable at each concentration, with consumption times usually extended four to sixfold. Overall, predator responses to purified alderenes were qualitatively and quantitatively comparable to those with live and dead slugs, or to positive controls using organic extracts, confirming that PKs comprise the antipredator defense.

Community effects of *Alderia* PKs

To test the hypothesis that *Alderia* PKs have effects beyond predator-prey interactions, we treated paired patches of the surface of a local mudflat with either the organic layer of *A. willowi* extract or an equal volume of carrier solvent as a control. The single dose simulated the release of PKs from *Alderia* during a mass die-off following peak densities in California. After 24 hours, infaunal community composition changed significantly in response to extract (Fig. 4 and Table 3). Most crustaceans were amphipods (primarily *Monocorophium* spp.) and benthic copepods. Abundance in extract-treated patches was significantly reduced by half or more for amphipods ($P < 0.01$; Fig. 4A) and copepods ($P < 0.001$; Fig. 4B and Table 3). The infaunal worm community was diverse, including five common polychaete genera and abundant nematodes, as well as less numerous oligochaetes and nemerteans (table S3). Treatment with *Alderia* metabolites significantly reduced annelid counts by about 25% compared to controls ($P < 0.01$; Fig. 4C), but nematode density was unaffected (Fig. 4D). Infaunal molluscs recovered in cores comprised juvenile bivalves and the heterobranch snail *Acteocina inculta*; abundance decreased more than 10-fold in response to *Alderia* extract, a highly significant change ($P < 0.001$; Fig. 4E and Table 3).

In contrast to the reduced infaunal abundance, extract-treated sediment contained six times more eggs of the California horn snail, *Cerithideopsis californica* ($P < 0.001$; Fig. 4F and Table 3). The horn snail was the most common and conspicuous invertebrate grazer sampled from the surface of the *Vaucheria* belt at the Salinas de San Pedro salt marsh when *Alderia* was absent, with densities ranging from 6.2 ± 3.5 to 16.7 ± 7.8 snails/m^2 in three surveys from March 2022 to April 2023. Eggs were mostly recovered in treatment cores proximal to vegetated areas where snails were abundant. Notably, eggs were sampled even in the winter deployment, whereas horn snails primarily reproduce in summer months.

To assess whether there was an overall effect of PKs on species richness, we calculated two indices of community diversity for all cores and compared mean diversity metrics for extract-treated versus control sediment. There was a borderline effect on species richness, with PK treatment reducing the Shannon-Wiener diversity index by more than 20% (Table 3), but no effect was seen on Simpson's Dominance index, which emphasizes the abundance of common taxa.

DISCUSSION

Abundant but inedible resources and estuarine food webs

Just as keystone species have a proportionately strong effect on community composition or function relative to their abundance, molecules

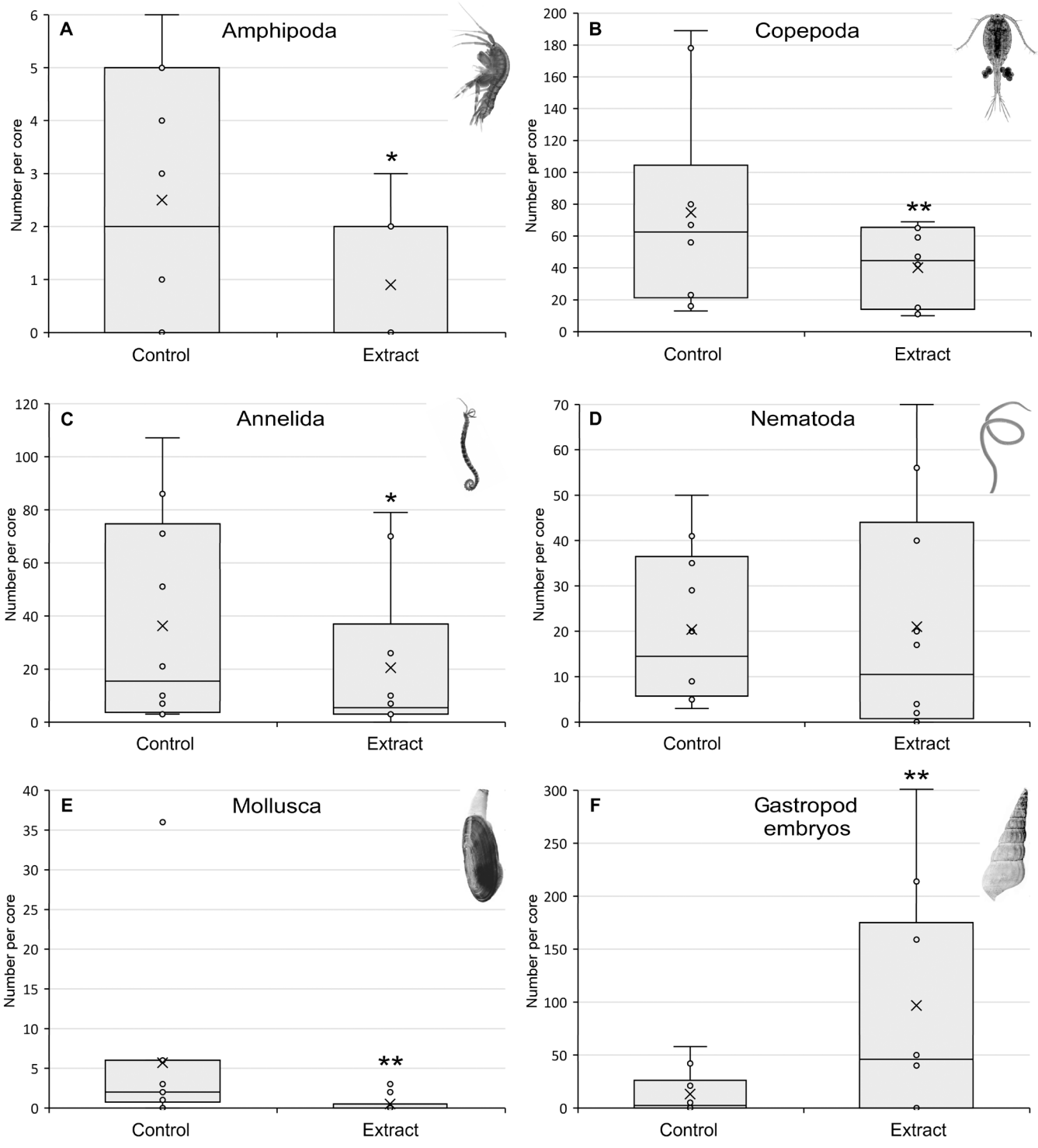

Fig. 4. Changes in infaunal abundance in response to alderenes applied to mud surface. Box-and-whisker plots show lower and upper quartiles of counts per core for: (**A**) amphipods; (**B**) copepods; (**C**) annelid worms; (**D**) nematodes; (**E**) adult molluscs; and (**F**) embryos of the snail *C. californica*. Horizontal lines are median values; "×" gives the mean ($N = 10$ cores). Data for summer and winter deployments were pooled. Asterisks denote treatments differing from controls based on generalized linear mixed-effects models; *$P < 0.01$; **$P < 0.001$.

Table 3. Results of generalized linear mixed-effect models (GLMMs) testing effects of *Alderia* extract on abundance of major taxa, and community diversity, in mudflat cores; boldfaced terms denote a significant change compared to controls.

Major taxa

Taxon	Estimate	SE	*Z*	*P*
Amphipoda	−1.022	0.384	−2.660	**0.008**
Copepoda	−0.623	0.062	−10.090	**$<2 \times 10^{-16}$**
Polychaeta	−0.227	0.086	−2.633	**0.008**
Nematoda	−0.019	0.096	−0.195	0.846
Mollusca (adult)	−2.398	0.467	−5.134	**2.84×10^{-7}**
Gastropoda (embryos)	1.808	0.084	21.500	**$<2 \times 10^{-16}$**

Community diversity

Diversity index	Estimate	SE	*Z*	*P*
Shannon-Wiener	0.136	0.077	1.779	0.075
Simpson's Dominance	0.041	0.039	1.050	0.294

of keystone significance are proposed to act at concentrations that are low relative to their ecological effects. Our findings support this hypothesis, showing that alderenes may play substantial but unrecognized roles in Northern Hemisphere estuaries. We characterized five new compounds and their biosynthetic enzymes from two grazers and demonstrated diverse effects of these metabolites on co-occurring predators as well as surface-dwelling and infaunal members of the mudflat community. This work provides a system for exploring how small molecules structure interaction networks, linking seemingly disconnected species with unexpected implications for food web dynamics and community diversity that may scale to ecosystem-level impacts.

Sea slugs are often discounted as major ecological players, but their impacts are increasingly recognized in disturbed systems including the loss of pelagic pteropods due to ocean acidification (*25*), alteration of infaunal communities by invasive cephalaspideans (*26*), and local removal of introduced algal species by sacoglossans (*27*). The deterrent metabolites of sea slugs may play a keystone role in ecosystems where slugs are impactful consumers and in turn, abundant potential prey items. *Alderia* spp. reach exceptional densities on temperate to boreal mudflats throughout the Northern Hemisphere. Along the U.S. West Coast, slugs comprise ~99% of animal biomass in the *Vaucheria* belt of many estuaries (*33*), with mean densities from 100 to 1000 slugs/m^2 and peak densities averaging 1000 to 3000 slugs/m^2 but exceeding 11,000/m^2 on some patches. Primary production by mats of the alga *Vaucheria* is potentially transferred to higher trophic levels almost exclusively through these dense herbivore populations. Mudflats may regularly have thousands of kilograms of slug biomass available to consumers. Molecules that prevent the consumption of slugs therefore regulate substantial energy flow within estuarine food webs, redirecting fixed carbon from algal mats to unexpected sinks.

Although the class of metabolites to which the alderenes belong has been known from related molluscs for 30 years, their ecological function was largely unexplored. The alderenes characterized here are structurally similar to PKs from other species in the ceratiform superfamily Limapontioidea but with a reduced pyrone ring not previously reported from sacoglossans (*22*, *43*, *47*–*51*). Most prior investigations tested slug PKs for toxicity against freshwater fish or in a hydra regeneration assay (*47*–*51*); few screened for bioactivity against co-occurring predators. Two large fish and two crab species ate *A.* cf. *modesta* (and other temperate sacoglossans), but the predators were more 20 times a slug's length, were not typical mudflat species, and were allowed to make repeated predation attempts for 3 days, potentially exhausting a slug's supply of defensive compounds (*46*). The tropical species *Cyerce nigricans* was unpalatable to fish and a specialized predator, the sea slug *Gymnodoris*; the crude organic extract of *Cyerce* contained a blend of cyercene-class γ-pyrones and deterred fish in the field (*52*). However two pure cyercenes did not inhibit feeding by wrasses in the laboratory (*53*). Thus, sacoglossan PKs were not previously known to repel ecologically relevant predators.

Here, we found that alderenes confer an effective chemical defense against small, co-occurring invertebrate and fish predators. Live *Alderia* spp. were unpalatable, secreting a mucus that predators found distasteful and that appeared to clog mouthparts and gills; slugs were attacked and often swallowed only to be spit out or dropped and survived all predation attempts. Dead slug tissue was also rejected by consumers unless organic compounds were removed first. Slug extracts conferred deterrent properties onto food pellets, and pure alderenes were sufficient to cause pellet rejection or aversive behaviors at concentrations as low as 0.025%, demonstrating that alderenes are responsible for the antifeedant properties of slugs.

Given their abundance in the high-productivity *Vaucheria* belt, *Alderia* spp. could represent an important food source for a range of invertebrate and vertebrate consumers. Instead, distasteful alderenes shunt energy away from predators that would otherwise consume *Alderia*. This represents a lost potential food resource for juvenile fish and invertebrates in important nursery habitat and potentially for nesting and migrating waterfowl if birds are similarly deterred. The fate of carbon fixed by *Vaucheria* is thus unclear. Dead or dying *Alderia* could be an important subsidy for mudflat scavengers and detritivores if decaying flesh is palatable, but slug tissue was equally repellent in predator assays. Given the high reproductive output of slugs (*36*), energy flow may be redirected to the nearshore plankton by the tidal export of *Alderia* larvae from mudflats, as slug embryos did not appear to be chemically defended. Given the wide distribution of *Alderia* and the high densities reached by slugs, the alderenes may thus have large-scale

impacts on estuarine food webs. Follow-up studies using isotopes to track nutrient flux through slug biomass are warranted to assess the ecosystem-level impacts of alderenes.

Keystone molecules affect mudflat communities

Our findings further indicate that alderenes substantially alter the composition of mudflat infauna in the *Vaucheria* belt, causing mobile infauna to leave sediment over one tidal cycle when exposed to ecologically realistic levels of alderenes. Treatment of surface sediment rapidly repelled four of five major groups of infauna, significantly reducing amphipod, copepod, annelid, and mollusc abundance. Only nematode roundworm abundance did not respond to slug compounds; nematodes exhibit broad tolerance to a range of extreme environments so may not be as susceptible to the repellant effects of alderenes as other taxa.

Even a single application of extract also had a near-significant effect on overall community diversity, indicating that slug compounds reduce diversity as well as abundance of mudflat meiofauna and macrofauna dwelling in the upper sediment layers. This strong response suggests that the steady release of alderenes in slug pedal mucus, or in bursts during episodic mass die-offs, may have large but unanticipated effects on the underlying community. The surface layers of mudflats are nutrient-rich but quickly become anoxic; many processes that occur in these sediments are subject to biodiversity-function effects, including bioturbation, nutrient recycling, and primary production (*54*–*56*). By reducing diversity and abundance of nearby infauna, dense slug populations may in turn affect such processes in complex ways that would not be predicted from traditional interaction networks. Microbial processes also profoundly affect the biogeochemistry of mudflats and may be affected by alderenes given the antibiotic properties of many PKs and the activity reported here; future work will examine the influence of slug compounds on the microbiome of sediments in the *Vaucheria* belt of estuaries.

In contrast to their deterrent effects on consumers and infauna, alderenes induced oviposition by a common co-occurring gastropod. The California horn snail preferentially spawned in the presence of alderenes, depositing egg cases that were rarely sampled in control cores. As horn snails primary graze benthic diatoms, they do not compete with *Alderia* for resources but may benefit from the local reduction in infauna triggered by repellent slug exudates. Sediment devoid of small invertebrates could represent a protected environment for vulnerable, encapsulated snail embryos during their prolonged period of benthic development, which lasts several weeks (*57*). Small crustaceans and worms may physically penetrate snail egg masses and allow entry by protists, directly and indirectly causing embryo mortality. Facilitation of snail reproduction by slug compounds could constitute a byproduct mutualism, with a shelled herbivore (*Cerithideopsis*) exploiting the chemical defense of a shell-less herbivore (*Alderia*) to increase the snail's reproductive success and hence fitness (*58*, *59*).

A keystone molecule should have effects disproportionate to its concentration, but no universal threshold for such a concentration exists. Slugs steadily secrete a suite of alderenes in their mucus secretions and must release larger pulses during mass die-offs; however, the compounds are never expected to be abundant in the environment, outside of the slug tissue. Even within slugs, concentrations of alderenes are notably low (0.1% for the major metabolite) compared to chemical defenses of many marine invertebrates, which can exceed 10% of dry weight (*58*). We propose that alderenes are candidate keystone molecules given their strong community-level effects on consumers, infauna, and surface grazers disproportionate to their concentration in the environment. These effects could potentially scale to ecosystem-level impacts given the network of affected species and broad distribution of *Alderia* spp., warranting further study of the ecological roles of molluscan PKs.

Broader implications for ecology and evolution

Although few marine heterobranchs reach the exceptional densities of *Alderia*, many invertebrates and algae are both locally abundant and rich in secondary metabolites (*22*, *60*–*62*). Allelopathy, in which the fitness of competing species is reduced by compounds released from a producing organism, has been well studied in terrestrial plants and some marine organisms (*63*, *64*). However, little attention has gone to "off-target" effects of allomones leaking into the environment on neighboring taxa that do not obviously interact or compete with the producing organism. Marine natural products are often highly bioactive and could alter invertebrate and microbial communities in adjacent sediments and on nearby surfaces; any suppression in local species could have cascading impacts on biodiversity-function effects. For instance, sponges are the most chemically rich animal group and could alter their environment via release of compounds into excurrent water flows or shed cells (*65*, *66*). Dense stands of chemically defended algae like *Caulerpa* could similarly affect many taxa sensitive to their metabolites. The extent to which chemistry weaves unexpected links in interaction networks thus warrants further study by marine ecologists.

The release of protective compounds also presents opportunities for by-product mutualisms to evolve, allowing resistant species to benefit from a chemical "shadow" and exploit the absence of susceptible species near a producing organism. As by-product mutualisms are thought to be one route to stable mutualisms and cooperative behavior (*58*, *59*), such relationships can have evolutionary consequences for species interactions. The potential benefits of "leaky" defenses for adjacent species thus deserve further exploration, both in the *Alderia*-*Vaucheria* system and in diverse other marine ecosystems. As abundant but unpalatable organisms also present models for the evolution of Batesian mimics, their chemistry may trigger a range of coevolutionary responses in associated species.

Recent work characterized the AFPKs, a previously unrecognized PK-synthesizing enzyme family that is widespread in bilaterian invertebrates but distinct from the canonical PK synthase enzymes found in animals and other domains of life (*43*–*45*). Clade Sacoglossa contains a private lineage of AFPK enzymes not detected in other gastropods, with distinct enzymes in photosynthetic (e.g., *Elysia*) versus nonphotosynthetic (e.g., *Alderia*) species (*44*, *45*). The AFPK genes identified here are among the first animal genes identified that produce a nonvenom chemical defense. Together, our findings thus far indicate sacoglossans evolved to produce longer-chain PKs (potential antioxidants and sunscreens) in photosynthetic species from an ancestral defensive role for AFPKs, making shorter-chain antifeedants like the alderenes (*44*, *45*). Comparing the AFPKs identified here, which biosynthesize smaller defensive molecules, to the AFPKs that generate bicyclic pyrones in *Elysia* spp. should inform our understanding of how metabolic pathways evolve novel functions. This work should also contribute to the development of the "keystone genes" concept (*67*) by linking variants in biosynthetic pathways to functional differences that change the properties of secreted chemicals, which in turn alter community structure and ecosystem function. Sacoglossans are sister to Pneumopulmonata, a hyperdiverse radiation that includes several lineages that evolved amphibious to fully terrestrial lives (*42*). As several air-breathing lineages (*Siphonaria* and *Onchidium*) also biosynthesize PKs (*68*), AFPK

enzymes may have facilitated gastropod transitions to semiterrestrial habitats and been important preadaptations underlying this explosive radiation. The role of this pathway in animal diversification also warrants further evolutionary study.

MATERIALS AND METHODS

Alderia abundance and population dynamics

Mean and peak densities for California populations of *A. willowi* and *A.* cf. *modesta* were estimated where the two species co-occur over a 100-km overlap zone along California's northern coast, from Bodega Harbor (northern range limit of *A. willowi*) to San Francisco Bay (southern limit of *A.* cf. *modesta*) (*38*). Monthly to quarterly surveys were performed in four estuaries within this overlap zone from December 2007 through March 2010, with supplemental surveys conducted before and afterward. Permanent 30-m transect lines were established along the *Vaucheria* belt parallel to tidal channels or the shoreline in Bodega Bay ($N = 2$), Tomales Bay ($N = 2$), Bolinas Lagoon ($N = 1$), and Mill Valley, San Francisco Bay ($N = 4$). Transect midpoints were recorded using a Garmin eTrex hand-held GPS unit. Temperature data loggers (Onset Corp; Bourne, MA) were attached to steel rebar anchored into the mudflat next to each transect at the same tidal height. Sensors were buried just under the mud surface to measure ecologically relevant temperatures experienced by *Alderia* at 5-min intervals. Daily maximum temperature of the mud surface was extracted for days when mass die-offs were observed.

Surveys were performed over one to two low tides by placing three to four quadrats (0.5 m^2) at 10-m intervals along a transect, removing all *Alderia* specimens by hand. A quadrat was surveyed by one to two collectors for up to 2 hours until 5 min passed without finding any slugs [full details in (*38*)]. Live slugs were typed to species by microscopic examination or for ambiguous specimens by multiplex polymerase chain reaction using custom primers to amplify species-diagnostic fragments differing in size for the mitochondrial *COI* gene). A haphazardly chosen subset of slugs from each transect ($N = 15$) were individually blotted dry and weighed to ±0.1 mg to assess size distributions and recruitment. A nonparametric Spearman's rank correlation was used to test for a relationship between abundance and size for each species in San Francisco Bay over the survey period.

Surveys for *A. willowi* were performed in 2022 and 2023 at two sites in Los Angeles, California, USA by establishing permanent transects and monitoring at monthly intervals as above. Surveys for ecologically relevant predators were also performed at these sites. Additional density data for *A. modesta* (Europe) and *A.* cf. *modesta* (Oregon, Russia) were taken from (*29*–*33*) and corrected for species identity (table S1). Linear regressions were performed for density, pooled for all *Alderia* spp., versus latitude (*33*). As the highest latitude site (Norway) also had the highest reported mean and peak densities, analyses were repeated excluding Norway as a potential outlier (fig. S13), both using raw counts and after natural log-transforming both variables. These sensitivity analyses indicated that removing Norway had little effect on the positive relationship between density and latitude, or on the goodness-of-fit as measured by R^2, and thus Norway was not driving the result.

To estimate total biomass of *Alderia* spp. in San Francisco Bay, biotic habitat classifications were downloaded from the West Coast USA Estuarine Biotic Habitat data layer of the Pacific Marine & Estuarine Fish Habitat Partnership (PMEP) (https://pacificfishhabitat.org/data/estuarine-biotic-habitat/). After subsetting the dataset for brackish emergent tidal marsh, the total habitat area (m^2) was quantified for (i) Mill Valley sites illustrated in Fig. 1, and (ii) San Francisco Bay. To estimate total biomass for an estuary, we then multiplied the habitat area by the average slug biomass per square meter calculated two ways. First, we multiplied mean density by mean wet weight during the peak season for *A.* cf. *modesta* (February to April) and *A. willowi* (August to October) from 2008 to 2010, to calculate biomass per square meter in peak season. Second, as an estimate of maximum peak biomass, we multiplied mean density by wet weight in the month with the highest recorded abundance for each species over the census period (*A.* cf. *modesta*, February 2010; *A. willowi*, October 2008).

Isolation and structure elucidation of alderenes

Live *A. willowi* were collected in November 2020 from San Pedro, CA under a Scientific Collecting Permit (SC 001494) from the CA State Department of Fish and Wildlife. Some slugs ($N = 7$) were individually preserved in EtOH, while two bulk collections ($N = 50$) of a combined 50-mg wet weight were frozen at −20°C before shipment on ice to the National Institutes of Health in Bethesda, MD. MS of extracts was conducted to establish the relative masses and fragmentation patterns of compounds and variability among individuals. Aliquots (750 μl) of single-slug extracts were dried under N_2 gas, resuspended in 200 μl of methanol, and centrifuged at 20,000*g* to remove particulates. The samples were analyzed on an Agilent 6545 quadrupole orthogonal acceleration–time of flight (Q-TOF) equipped with an Agilent 1290 Infinity II Quaternary UHPLC system, ZORBAX Eclipse Plus C18 column (50 mm by 2.1 mm, 1.8 μm), and Dual AJS ESI source. Samples were eluted with a 5 to 90% acetonitrile gradient over 9 min (mobile phase A, 0.1% formic acid in water; mobile phase B, acetonitrile) with a mass range of 100 to 1700 *m/z*.

Compounds **1** to **5** were isolated as follows: 150 whole *A.* cf. *modesta* (2.3-g wet weight, collected on 31 October 2020 from San Pablo Bay, 38°09′07.6″N, 122°26′12.4″W) were extracted five times with acetone under sonication in 5-min intervals. The extract was evaporated under vacuum to produce an aqueous suspension, which was taken up in brine (10 ml) and extracted three times with dichloromethane (10 ml). The organic phase was evaporated under reduced pressure to afford 90 mg of green oil. This material was loaded onto HP20ss and the resin bed washed with water, then methanol, and, finally, acetone (20 ml each), and the eluent evaporated under reduced pressure. The acetone fraction contained lipids including sterols; the methanol fraction produced gold-colored oil (29 mg), with PKs the main compounds noticeable by NMR analysis. The methanol fraction was separated by semi-preparative HPLC performed on a Hitachi Primaide system equipped with a photodiode array detector (1110 pump and 1430 DAD) and a Phenomenex Luna Phenyl-Hexyl 100 Å column (10 mm by 250 mm, 5 μm), providing compounds **1** (570 μg), **2** (180 μg), **3** (350 μg), **4** (80 μg), and **5** (50 μg).

IR spectra were recorded on a Nicolet iS5 Fourier transform IR spectrometer operating in attenuated total reflectance (ATR) mode (Thermo Fisher Scientific). Optical rotations were recorded on a PerkinElmer Model 343 polarimeter). High-resolution mass spectra were obtained using a Waters Acquity UPLC linked to a Waters Xevo G2-XS Q-TOF. ^{1}H NMR and ^{13}C NMR spectra were recorded on a Varian iNOVA 500 (^{1}H 500 MHz) NMR spectrometer equipped with a 3-mm Nalorac MDBG probe, or a Varian iNOVA 600 (^{1}H 600 MHz) NMR spectrometer equipped with a 5-mm Varian inverse cold probe operated using VNMRJ 4.2. Data were processed and analyzed using MestreNova 9.1.0. Chemical shifts were

referenced to the solvent residual proton for ^{1}H NMR (δ 7.25 for $CDCl_3$) and the ^{13}C signal for ^{13}C NMR (δ 77.2 for $CDCl_3$).

(i) Alderene **A** (**1**): Clear oil; $[\alpha]_D^{20}$ +43.8 (*c* 0.160, $CHCl_3$); UV (MeOH) λ_{max} (log ε) 232 (4.2); ECD (0.35 mM, MeCN), λ_{max} (Δε) 219 (+19), 260 (−8.3) nm; IR (ATR) ν_{max} 2916, 1711, 1616, 1458, 1360, 1290, 1272, 1223, 1090, 1017; NMR see Table 1; HRESIMS *m/z* 259.1322 (calculated for $C_{14}H_{20}O_3Na^+$, 259.1305).

(ii) Alderene **B** (**2**): Clear oil; $[\alpha]_D^{20}$ +36.2 (*c* 0.051, $CHCl_3$); UV (MeOH) λ_{max} (log ε) 234 (3.3); ECD (0.11 mM, MeCN), λ_{max} (Δε) 259 (+5.3) nm; IR (ATR) ν_{max} 2923, 1713, 1615, 1459, 1362, 1291, 1271, 1220, 1064, 1015; NMR see Table 1; HRESIMS *m/z* 273.1484 (calculated for $C_{15}H_{22}O_3Na^+$, 273.1462).

(iii) Alderene **C** (**3**): Clear oil; $[\alpha]_D^{20}$ +31.0 (*c* 0.100, $CHCl_3$); UV (MeOH) λ_{max} (log ε) 231 (4.1); ECD (0.21 mM, MeCN), λ_{max} (Δε) 223 (+24), 263 (−2.4) nm; IR (ATR) ν_{max} 2922, 1713, 1617, 1458, 1361, 1290, 1272, 1223, 1065, 1017; NMR see Table 1; HRESIMS *m/z* 273.1483 (calculated for $C_{15}H_{22}O_3Na^+$, 273.1462).

(iv) Alderene **D** (**4**): Clear oil; $[\alpha]_D^{20}$ +16.7 (*c* 0.024, $CHCl_3$); UV (MeOH) λ_{max} (log ε) 235 (3.5); ECD (0.06 mM, MeCN), λ_{max} (Δε) 257 (+8.4); IR (ATR) ν_{max} 2922, 2852, 1735, 1685, 1647, 1559, 1458, 1379, 1321, 1092; NMR see Table 1; HRESIMS *m/z* 287.1639 (calculated for $C_{16}H_{24}O_3Na^+$, 287.1639).

(v) Alderene **E** (**5**): Clear oil; NMR see Table 1; HRESIMS m/z 259.1323 (calculated for $C_{14}H_{20}O_3Na^+$, 259.1305).

ECD spectral prediction

Alderene **1** was determined to be of the (5*S*, 6*R*) configuration by comparison of predicted and experimental ECD spectra. Briefly, a conformer search was performed manually using a combination of Merck molecular force field (MMFF) calculations and comparison to NMR data, primarily NOESY. Four major, nondegenerate conformers were identified including two pyrone conformational states (with trans side chain and methyl groups either pseudo-equatorial or pseudo-axial) and two diene conformational states (*S*-cis configured *E*,*E*-diene system twisted out of plane plus or minus 45°). These were optimized using DFT with a B3LYP functional and a 6-31G(d) basis set in Gaussian v.16 (*69*). Electronic and thermal energy corrections were calculated at 25°C using frequency calculations. The ECD spectra were calculated using TD-DFT at the previous level of theory along with an acetonitrile conductor-like polarizable continuum model (CPCM) solvent model. Gaussview v.6 was used to plot and export the ECD spectra, which were then Boltzmann weighted and averaged. A correction factor (+25 nm) was added to account for systematic errors in computed transition energies.

Metabolite quantification

A collection of *A*. cf. *modesta* (20.3 g) was separated into four groups with a mean wet weight of 5.01 g ± 0.48 SD. Each group was extracted in an identical manner by sonicating in acetone (15 ml) three times and pooling extractions for a group, yielding four replicate extracts of ~45 ml each. The samples were diluted to exactly 50 ml in a volumetric flask with acetone. An aliquot (20 μl) of each sample was diluted in methanol (200 μl) in a glass insert and analyzed by LC-MS. The peak for compound **1** (R_t 4.01 min) was integrated in each total ion chromatogram and the area compared to a standard curve (prepared by analyzing solutions of purified **1** in twofold serial dilution starting at 50 μg/ml). The concentration of **1** in each sample was calculated and determined to be on average 919 parts per million (ppm) (±0.00938 ppm SD), or 0.09% wet weight.

Only compounds **1** and **5** were detected in *A. willowi,* at approximately the same concentrations as in *A*. cf. *modesta* relative to tissue weight. By integrating under the peaks on LC-MS traces of both species, **1** and **5** were about sixfold less concentrated in extracts of individual *A. willowi* (1.2 mg in mean weight), roughly six times smaller than *A*. cf. *modesta* used for metabolite quantification (8-mg mean weight). In both species, **1** was typically three times more abundant than **5**.

Identification and phylogenetic relationships of biosynthetic AFPKs

Total RNAs were extracted from live *A*. cf. *modesta* (two pools of 10 slugs each) using TRIzol extraction (Invitrogen), and DNA was removed using the DNA-free DNA Removal Kit (Invitrogen). Illumina sequencing was performed at the Huntsman Cancer Institute High Throughput Genomics Core. The Illumina TruSeq Stranded mRNA Kit was used for library preparation with unique dual indexes and the library sequenced using a NovaSeq S4 Reagent Kit to generate 150–base pair paired end reads and 2500 M read pairs total. The raw reads were trimmed using Trimmomatic and trimmed reads de novo assembled using SPAdes (*70*). The transcriptome was searched by tblastn using sacoglossan AFPK protein sequences as queries (*43*). Phylogenetic analysis was performed using a previously described set of selected PKS, FAS, and AFPK protein sequences (*43*). An initial alignment was made and aligned sequences trimmed to about 1300 amino acid residues. A second alignment was generated using Geneious (alignment type, global with free end gaps; cost matrix, Blosum 45; gap open penalty, 12; gap extension penalty, 3; refinement iterations, 3) and analyzed by maximum likelihood using the IQ-TREE web tool (Los Alamos National Laboratory) with the following options: number of sequences, 42; sequence type a substitution model, amino acids, Blosum62; rate heterogeneity, none; state frequency, estimated by ML; bootstrap branch support, none; single-branch test, none; tree search, perturbation strength 0.5, # of unsuccessful iterations to stop = 100; root tree, none (*71*). Transcripts were quantified using Salmon (*72*). Values reported are the average of two biological replicates.

Antifeedant assays: Whole slugs and egg masses

Three generalist predators co-occurring with *Alderia* in Californian estuaries were used: the arrow goby *C. ios*, polychaete worm *N. arenaceodentata*, and lined shore crab *P. crassipes*. Fish and crabs were collected by hand using a small net under permit SC 001494. Polychaete worms were purchased from Aquatic Toxicology Support LLC (Bremerton, WA). Slugs were hand-collected in the field and maintained on algae in plastic bins in an incubator at 16°C on a 14:10 light:dark cycle. Live slugs used in experiments were housed for 1 week after a predation trial to assess delayed mortality in glass dishes in 500 ml of aerated, 24‰ artificial sea water (ASW), with algae changed every 2 days. Predators were housed in individual containers and acclimated for 1 week before trials. Fish were individually maintained in tanks with 19 liter of ASW following all federal and institutional guidelines for vertebrate work (IACUC protocol number 1013-01). Crabs and worms were housed in individual plastic bins with 100 or 500 ml ASW, respectively, and appropriate substrate. Seawater was changed three times/week. Predators were fed squid flesh every 2 days, and worms were also fed dried algae (*Enteromorpha*). Prey items were offered via pipet, and each predator was used only once per trial; predators that rejected any prey item were then offered squid to confirm willingness to feed.

In assays with live slugs, fish ($N = 10$), crabs ($N = 9$), and worms ($N = 20$) were used after 2 days of starvation to ensure readiness to feed. In separate trials, each predator was individually offered a live *A.* cf. *modesta* or *A. willowi,* and a control piece of squid of equivalent wet weight and volume to the slug. Predators were offered a slug or control in a randomized order; any that rejected a slug were subsequently offered squid to confirm that they were willing to feed. Trials were observed and recorded for 5 min from the time a prey item was introduced, scoring time to fully consume a meal and number of attacks on a prey item. Because of nonnormality of the data, time and number of attacks were compared between treatment and controls using nonparametric sign tests, while the proportion of live slugs versus controls consumed was compared using Fisher's exact test (*61*–*62*, *73*).

Comparable assays were then run testing dead slugs to determine whether active mucus secretion was an essential component of slug defense. Slugs were flash-frozen at −80°C overnight and then thawed for 1 hour. Control pieces of squid were frozen/thawed in parallel. Fish and crabs ($N = 10$ each) were offered a frozen/thawed specimen of *A. willowi* or squid in random order as described above. To test whether solvent extraction (removing potential nonpolar feeding deterrents) rendered slug tissue palatable, frozen slugs were incubated in acetone for 24 hours and then rehydrated in seawater before trials. A control piece of squid of equivalent wet weight and volume to each individual slug was extracted and rehydrated in parallel to ensure that feeding cues were not removed by acetone extraction. Fish ($N = 10$), crabs ($N = 9$), and worms ($N = 10$) were offered an acetone-extracted slug (separate trials for each *Alderia* species) and a control in random order. The time spent consuming prey items met assumptions of normality and was compared using independent *t* tests for trials on extracted slugs.

To test whether slugs incorporate defensive compounds into egg masses, fish and crabs ($N = 10$ each) were offered an egg mass of *A. willowi* and a control piece of squid in random order, and the proportion of each consumed was compared by Fisher's exact test for each predator. A second trial was done cutting egg masses in half to expose the gelatinous string of embryos to assess whether fish ($N = 10$) would consume embryos more readily without having to bite through the outer casing of the egg mass.

Antifeedant assays: Slug extracts and pure alderenes

Bioassay-guided fractionation was used to identify the compound(s) responsible for the deterrent properties of slugs. Collections of *A.* cf. *modesta* and *A. willowi* ($N = 50$ to 100 slugs per species, 100-mg wet weight total per species) were separately extracted three times sequentially with 50 ml of acetone for 24 hours. Combined extracts of each species were concentrated by rotary evaporation and partitioned three times between ethyl acetate and water; the organic layer was concentrated and dried (~11 mg per species). An artificial food for testing extract palatability was made by homogenizing squid mantle in water at a 1:1 ratio by mass and adding sodium alginate to yield a 2% final concentration (*59*, *60*). The mass of squid tissue homogenized was equal to the mass of sea slug tissue extracted to ensure that the extract was tested in proportion to the natural concentration in slugs; volumes of tissue were also equivalent. We homogenized 89 mg of squid mantle plus 2 mg of sodium alginate in 0.1 ml of water for each *Alderia* sp.; the corresponding organic extract (11 mg) of each species was resolubilized in 50 μl of acetone and added to the homogenate. The ingredients were mixed in a 1-ml syringe and extruded into 0.25 M $CaCl_2$ to solidify into slug-sized (4 mm) treatment pellets. Solvent-only control pellets were made with 100 mg of squid mantle blended in 0.1 ml of water with 2 mg of sodium alginate and 50 μl of acetone added. After 2 days without food, each predator was offered an extract-treated pellet versus a control pellet and the proportion of pellets consumed compared using Fisher's exact test; separate trials were run for each *Alderia* sp. × predator combination.

A collection of *A. willowi* made in November 2020 from San Pedro, CA ($N = 100$ slugs; 99-mg wet weight) was frozen at −20°C, extracted in acetone, and partitioned into organic and aqueous layers. The organic layer was further partitioned between a methanol fraction, highly enriched in PKs (~95% pure by NMR), and a hexane layer containing sterols and fats (fig. S7). Preliminary feeding assays indicated that the deterrent effect of *Alderia* extract was contained in the PK-enriched methanol fraction and not the hexane layer. To confirm that alderenes were responsible for the antipredator activity of extracts, pure compounds **1** and **5** were bioassayed following structure elucidation. A collection of 150 *A.* cf. *modesta* (2.3-g wet weight) in March 2021 yielded a semipurified extract (29 mg) that was mostly PK by NMR. Purification by HPLC yielded 1.2 mg of pure PKs ranging from 80 to 570 μg per metabolite for bioassays. Alderenes **1** and **5** were tested in crab and fish assays at 0.025, 0.05, and 0.1% of tissue weight in pellets, or approximately 25, 50, and 100% of the natural concentration of alderene **1** estimated for *A.* cf. *modesta* by wet weight. A stock solution was prepared by homogenizing 100 mg of squid mantle tissue in 0.1 ml of water with 2 mg of sodium alginate. The appropriate amount of each compound was taken up in 10 μl of methanol and added to 40 μl of homogenate and then mixed with $CaCl_2$ solution to yield 10 food pellets containing 10 μg (0.025%), 20 μg (0.05%), or 40 μg (0.1%) of each alderene. Consumption was scored and compared to both positive and negative controls prepared in parallel during 5 min trials. Negative controls were solvent-only control pellets; positive controls incorporated crude extract prepared freshly and made at 25, 50, or 100% on a per-weight basis.

Because of limited quantities of pure compounds, pellets were smaller than in previous assays and predators were more likely to ingest at least a portion of treatment pellets. We therefore recorded 5-min feeding trials on video and scored behaviors indicating deterrence. For crabs, such behaviors included time processing pellets during feeding attempts, time spent removing particles or mucus from mouthparts, proportion of individuals that rubbed or pressed mouthparts against substrate, number of cheliped movements into the mouth during feeding attempts, and number of cheliped movements pulling from the mouth after feeding. For fish, behaviors included the number of times a pellet was regurgitated during feeding attempts, the initial delay before a feeding attempt was made, and total prey-handling time including repeated regurgitation or bites to break pellets into smaller pieces. Fish behaviors could only be tested at 25 and 50% of natural concentrations due to limited quantities of pure alderenes. Response variables recorded as time or number were compared for treatment pellets versus controls using a nonparametric paired Sign test (both predators); the proportion of crabs pressing mouthparts against the substrate was compared for treated versus control pellets using Fisher's exact test.

Field assays of community response to alderenes

Manipulative field experiments were performed at the Salinas de San Pedro salt marsh to assess the response of mudflat community

species to alderenes. In pilot surveys, dominant infauna were small crustaceans (amphipods and benthic copepods), diverse worms, and molluscs. The only common invertebrate on the mud surface in the *Vaucheria* belt was the California horn snail, *C. californica*, but snails were more abundant among cordgrass higher in the marsh. We assessed the response of the mudflat community in two trials performed in June and December 2022. *Alderia* had been present year-round in this marsh before 2018, but at the time of each 2022 field trial, no *Alderia* were detected in surveys for >2 months during a prolonged population crash. Specimens of *A. willowi* ($N = 75$) were collected from the Golden Shores site (Long Beach, CA), weighed (June: 519 mg; December: 467 mg), and extracted in acetone twice for 24 hours. Pooled extracts were dried by rotary evaporation and then partitioned three times between ethyl acetate and water; organic layers were dried and weighed (June: 3.3 mg; December: 3.0 mg).

Slug extracts were then applied to the mud surface to simulate the release of PKs in slug mucus or during mass die-offs following peak annual densities measured in northern California. The extract was redissolved in 1 ml of methanol and divided into five aliquots. Replicate pairs ($N = 5$) of treatment and control patches were marked at 3-m intervals along a permanent transect. Each patch was a circle on the mud surface to which an aliquot of extract (200 µl) was applied by micropipetting extract onto the mud surface, or an equivalent application of 200 µl or methanol (paired control patches). Extract delivered the organic-layer PKs from 15 slugs spread over ~40 cm^2 to approximate observed die-off events. Solvent evenly dispersed over the mud and was quickly absorbed. After 24 hours (two high tides), each patch was cored to 2.5-cm depth using a premarked 5 cm–by–12 cm cellulose acetate butyrate plastic liner tubes for infaunal community analysis (*74*). Cores (~50 ml of sediment) were fixed in 5% neutral buffered formalin for 2 days, then passed over a 1-mm prefilter, and organisms retained on stacked 500- and 300-µm mesh sieves, transferred to 70% ethanol and stained with Rose Bengal dye (*75*, *76*). Macrofauna and meiofauna were separated under a dissecting microscope and identified to the lowest taxonomic group possible following (*77*). Crustaceans were treated as infaunal as they were rarely observed on exposed mud patches by stereoscopic examination but could be surface-active when immersed at high tide. Annelids were identified to the genus level in collaboration with L. Harris and archived in the Los Angeles County Museum of Natural History collection.

Field experiments included a fixed effect, paired treatment versus control cores, as well as a random effect of trial season. The R package lme4 (*78*) was used to create generalized linear mixed-effect models (GLMM) with the glmer function, to compare mean abundance for each taxonomic group. The Poisson distribution was used for GLMMs as the response variable (abundance) was count data. Analyses were run in R 4.2.3 (*79*).

To determine whether community diversity differed between the treatment and control cores, the Shannon-Wiener Index and Simpson's Dominance Index were calculated for each core. Shannon's index is an information statistic index that assumes that all species were represented and randomly sampled in a community. Simpson's index is a dominance index that accounts for both the number of species present and the relative abundance of each species in the community. Mean values were compared between treatment and control cores using the glmer function with a gamma distribution, as the response variables were continuous and nonnegative.

Supplementary Materials

The PDF file includes:

Figs. S1 to S13
Tables S1 to S3
Legends for movies S1 to S3
Supplementary NMR Data
Computational Data

Other Supplementary Material for this manuscript includes the following:

Movies S1 to S3

REFERENCES AND NOTES

1. R. T. Paine, Food web complexity and species diversity. *Am. Nat.* **100**, 65–75 (1966).
2. R. T. Paine, A note on trophic complexity and community stability. *Am. Nat.* **103**, 91–93 (1969).
3. M. Power, D. Tilman, J. Estes, B. A. Menge, W. Bond, L. Mills, G. Daily, J. Castilla, J. Lubchenco, R. T. Paine, Challenges in the quest for keystones: Identifying keystone species is difficult but essential to understanding how loss of species will affect ecosystems. *Bioscience* **46**, 609–620 (1996).
4. F. Jordan, Keystone species and food webs. *Philos. Trans. R. Soc. Lond. B Biol. Sci.* **364**, 1733–1741 (2009).
5. G. Pohnert, M. Steinke, R. Tollrian, Chemical cues, defense metabolites and the shaping of pelagic interspecific interactions. *Trends Ecol. Evol.* **22**, 198–204 (2007).
6. M. E. Hay, Marine chemical ecology: Chemical signals and cues structure marine populations, communities, and ecosystems. *Ann. Rev. Mar. Sci.* **1**, 193–212 (2009).
7. M. E. Hay, J. Kubanek, Community and ecosystem level consequences of chemical cues in the plankton. *J. Chem. Ecol.* **28**, 2001–2016 (2002).
8. R. P. Ferrer, R. K. Zimmer, Community ecology and the evolution of molecules of keystone significance. *Biol. Bull.* **223**, 167–177 (2012).
9. R. P. Ferrer, R. K. Zimmer, Molecules of keystone significance: Crucial agents in ecology and resource management. *Bioscience* **63**, 428–438 (2013).
10. R. K. Zimmer, R. P. Ferrer, Neuroecology, chemical defense, and the keystone species concept. *Biol. Bull.* **213**, 208–225 (2007).
11. R. Kvitek, C. Bretz, Harmful algal bloom toxins protect bivalve populations from sea otter predation. *Mar. Ecol. Prog. Ser.* **271**, 233–243 (2004).
12. G. V. Wolfe, The chemical defense ecology of marine unicellular plankton: Constraints, mechanisms, and impacts. *Biol. Bull.* **198**, 225–244 (2000).
13. M. S. Savoca, G. A. Nevitt, Evidence that dimethyl sulfide facilitates a tritrophic mutualism between marine primary producers and top predators. *Proc. Natl. Acad. Sci. U.S.A.* **111**, 4157–4161 (2014).
14. K. L. Van Alstyne, M. Puglisi, DMSP in marine macroalgae and macroinvertebrates: Distribution, function, and ecological impacts. *Aquat. Sci.* **69**, 394–402 (2007).
15. F. Sánchez-Piñero, G. A. Polis, Bottom-up dynamics of allochthonous input: Direct and indirect effects of seabirds on islands. *Ecology* **81**, 3117–3132 (2000).
16. W. H. Hol, A. Van Veen, Pyrrolizidine alkaloids from *Senecio jacobaea* affect fungal growth. *J. Chem. Ecol.* **28**, 1763–1772 (2002).
17. J. R. Trigo, Effects of pyrrolizidine alkaloids through different trophic levels. *Phytochem. Rev.* **10**, 83–98 (2011).
18. E. M. Hill, L. A. Robinson, A. Abdul-Sada, A. J. Vanbergen, A. Hodge, S. E. Hartley, Arbuscular mycorrhizal fungi and plant chemical defense: Effects of colonisation on aboveground and belowground metabolomes. *J. Chem. Ecol.* **44**, 198–208 (2018).
19. K. M. Dahlstrom, D. L. McRose, D. K. Newman, Keystone metabolites of crop rhizosphere microbiomes. *Curr. Biol.* **30**, R1131–R1137 (2020).
20. K. Dettner, Toxins, defensive compounds and drugs from insects in K. H. Hoffmann, Ed., *Insect Molecular Biology and Ecology*, (CRC Press, 2014).
21. G. Cimino, M. Ghiselin, Chemical defense and the evolution of opisthobranch gastropods. *Proc. Calif. Acad. Sci.* **60**, 175–422 (2009).
22. J. R. Pawlik, Marine invertebrate chemical defenses. *Chem. Rev.* **93**, 1911–1922 (1993).
23. R. Valles-Regino, P. Mouatt, L. H. Yee, K. Benkendorff, Ocean warming and heat stress impact molecules of keystone significance in a predatory marine gastropod. *Front. Mar. Sci.* **9**, 830425 (2022).
24. D. Obermann, B. Ulf, H. Wägele, Incorporated nematocysts in *Aeolidiella stephanieae* (Gastropoda, Opisthobranchia, Aeolidoidea) mature by acidification shown by the pH sensitive fluorescing alkaloid Ageladine A. *Toxicon* **60**, 1108–1116 (2012).
25. N. Bednaršek, C. Harvey, I. Kaplan, R. Feely, J. Možina, Pteropods on the edge: Cumulative effects of ocean acidification, warming, and deoxygenation. *Prog. Oceanogr.* **145**, 1–24 (2016).
26. D. B Cadien, J. Ranasinghe, "Invaders in the open sea: Establishment of the New Zealand snail *Philine auriformis* in Southern California coastal waters" in *Annual Report of the Southern California Coastal Water Research Project*, S. B. Weisberg, D. Elmore, Eds. (Southern California Coastal Water Research, 2003).
27. C. D. Trowbridge, C. D. Todd, Host-plant change in marine specialist herbivores: Ascoglossan sea slugs on introduced macroalgae. *Ecological monographs* **71**, 219–243 (2001).

28. C. E. Kicklighter, M. Kamio, L. Nguyen, M. W. Germann, C. D. Derby, Mycosporine-like amino acids are multifunctional molecules in sea hares and their marine community. *Proc. Natl. Acad. Sci. U.S.A.* **108**, 11494–11499 (2011).
29. C. den Hartog, Distribution and ecology of the slugs *Alderia modesta* and *Limapontia depressa* in the Netherlands. *Beaufortia* **7**, 15–36 (1959).
30. U. Seelemann, Rearing experiments on the amphibian slug *Alderia modesta*. *Helgol. Wiss. Meeresunters.* **15**, 128–134 (1967).
31. W. Vader, *Alderia modesta* (Gastropoda, Sacoglossa) in northern Norway. *Fauna Norv.* **2**, 41–46 (1981).
32. A. V. Chernyshev, E. M. Chaban, The first findings of *Alderia modesta* (Lovén, 1844) (Opistobranchia, Ascoglossa) in the Sea of Japan. *Ruthenica* **14**, 131–134 (2005).
33. C. D. Trowbridge, Local and regional abundance patterns of the ascoglossan (=sacoglossan) opisthobranch *Alderia modesta* (Lovén, 1844) in the northeastern Pacific. *Veliger* **36**, 303–310 (1993).
34. R. A. Ellingson, P. J. Krug, Evolution of poecilogony from planktotrophy: Cryptic speciation, phylogeography and larval development in the gastropod genus *Alderia*. *Evolution* **60**, 2293–2310 (2006).
35. P. J. Krug, R. A. Ellingson, R. Burton, A. A. Valdés, A new poecilogonous species of sea slug (Opisthobranchia: Sacoglossa) from California: Comparison with the planktotrophic congener *Alderia modesta* (Lovén, 1844). *J. Moll. Stud.* **73**, 29–38 (2007).
36. P. J. Krug, Poecilogony and larval ecology in the gastropod genus *Alderia*. *Am. Malacol. Bull.* **23**, 99–111 (2007).
37. C. D. Trowbridge, Population structure of two common species of ascoglossan (= sacoglossan) opisthobranches on the central coast of Oregon USA. *Veliger* **36**, 99–106 (1993).
38. M. N. Garchow, "*Population Dynamics at the Range Boundary between Sister Species of the Estuarine Sea Slug genus Alderia: Role of the Physical Environment versus Larval Supply*," (California State Univ., 2010).
39. P. J. Krug, E. Shimer, V. A. Rodriguez, Differential tolerance and seasonal adaptation to temperature and salinity stress at a dynamic range boundary between estuarine gastropods. *Biol. Bull.* **241**, 105–122 (2021).
40. S. Rosa, J. Granadeiro, C. Vinagre, S. França, H. Cabral, J. M. Palmeirim, Impact of predation on the polychaete *Hediste diversicolor* in estuarine intertidal flats. *Estuar. Coast. Shelf Sci.* **78**, 655–664 (2008).
41. M. Sheaves, R. Baker, I. Nagelkerken, R. M. Connolly, True value of estuarine and coastal nurseries for fish: Incorporating complexity and dynamics. *Estuar. Coasts* **38**, 401–414 (2015).
42. P. J. Krug, S. A. Caplins, K. Algoso, K. Thomas, Á. A. Valdés, R. Wade, N. L. Wong, D. J. Eernisse, K. M. Kocot, Phylogenomic resolution of the root of Panpulmonata, a hyperdiverse radiation of gastropods: New insight into the evolution of air breathing. *Proc. Roy. Soc. B* **289**, 20211855 (2022).
43. J. Torres, Z. Lin, J. Winter, P. J. Krug, E. W. Schmidt, Animal biosynthesis of complex polyketides in a photosynthetic partnership. *Nat. Commun.* **11**, 2882 (2020).
44. F. Li, Z. Lin, P. J. Krug, J. L. Catrow, J. E. Cox, E. W. Schmidt, Animal FAS-like polyketide synthases produce diverse polypropionates. *Proc. Natl. Acad. Sci. U.S.A.* **120**, e2305575120 (2023).
45. Z. Lin, F. Li, P. J. Krug, E. W. Schmidt, The polyketide to fatty acid transition in the evolution of animal lipid metabolism. *Nat. Commun.* **15**, 236 (2023).
46. C. D. Trowbridge, Defensive responses and palatability of specialist herbivores: Predation on NE Pacific ascoglossan gastropods. *Mar. Ecol. Prog. Ser.* **105**, 61–70 (1994).
47. A. Cutignano, A. Fontana, L. Renzulli, G. Cimino, Placidenes C-F, novel α-pyrone propionates from the Mediterranean sacoglossan *Placida dendritica*. *J. Nat. Prod.* **66**, 1399–1401 (2003).
48. M. Ciavatta, E. Manzo, G. Nuzzo, G. Villani, G. Cimino, J. Cervera, M. Malaquias, M. Gavagnin, Aplysiopsenes: An additional example of marine polyketides with a mixed acetate/propionate pathway. *Tetrahedron Lett.* **50**, 527–529 (2009).
49. R. R. Vardaro, V. Di Marzo, A. Marin, G. Cimino, α-and γ-Pyrone-polypropionates from the Mediterranean ascoglossan mollusc *Ercolania funerea*. *Tetrahedron* **48**, 9561–9566 (1992).
50. R. R. Vardaro, V. Di Marzo, A. Crispino, G. Cimino, Cyercenes, novel polypropionate pyrones from the autotomizing Mediterranean mollusc *Cyerce cristallina*. *Tetrahedron* **47**, 5569–5576 (1991).
51. V. Di Marzo, A. Marin, R. R. Vardaro, L. De Petrocellis, G. Villani, G. Cimino, Histological and biochemical bases of defense mechanisms in four species of Polybranchioidea ascoglossan molluscs. *Mar. Biol.* **117**, 367–380 (1993).
52. V. Roussis, J. R. Pawlik, M. E. Hay, W. Fenical, Secondary metabolites of the chemically rich ascoglossan *Cyerce nigricans*. *Experientia* **46**, 327–329 (1990).
53. M. E. Hay, J. R. Pawlik, J. Duffy, W. Fenical, Seaweed-herbivore-predator interactions: Host-plant specialization reduces predation on small herbivores. *Oecologia* **81**, 418–427 (1989).
54. A. M. Karlson, F. J. Nascimento, J. Näslund, R. Elmgren, Higher diversity of deposit-feeding macrofauna enhances phytodetritus processing. *Ecology* **91**, 1414–1423 (2010).
55. E. N. Ieno, M. Solan, P. Batty, G. J. Pierce, How biodiversity affects ecosystem functioning: Roles of infaunal species richness, identity and density in the marine benthos. *Mar. Ecol. Prog. Ser.* **311**, 263–271 (2006).
56. R. Pinto, V. N. de Jonge, J. C. Marques, Linking biodiversity indicators, ecosystem functioning, provision of services and human well-being in estuarine systems: Application of a conceptual framework. *Ecol. Indic.* **36**, 644–655 (2014).
57. M. S. Race, Field ecology and natural history of *Cerithidea californica* (Gastropoda: Prosobranchia) in San Francisco Bay. *Veliger* **24**, 18–27 (1981).
58. J. L. Sachs, U. G. Mueller, T. P. Wilcox, J. J. Bull, The evolution of cooperation. *Q. Rev. Biol.* **79**, 135–160 (2004).
59. G. Chomicki, E. T. Kiers, S. S. Renner, The evolution of mutualistic dependence. *Annu. Rev. Ecol. Evol. Syst.* **51**, 409–432 (2020).
60. C. J. Freeman, D. F. Gleason, Chemical defenses, nutritional quality, and structural components in three sponge species: *Ircinia felix*, *I. campana*, and *Aplysina fulva*. *Mar. Biol.* **157**, 1083–1093 (2010).
61. J. R. Pawlik, Antipredatory defensive roles of natural products from marine invertebrates in *Handbook of Marine Natural Products*, E. Fattorusso, W. H. Gerwick, O. Taglialatela-Scafati (eds), (Springer, 2012).
62. M. E. Hay, J. J. Stachowicz, E. Cruz-Rivera, S. Bullard, M. S. Deal, N. Lindquist, Bioassays with marine and freshwater macroorganisms in *Methods in chemical ecology*, K. F. Haynes, J. G. Millar (eds), (Chapman & Hall, 1998).
63. M. J. Reigosa, N. Pedrol, L. González (eds) *Allelopathy: A physiological process with ecological implications* (Springer, 2006).
64. F. V. Ribeiro, B. A. da Gama, R. C. Pereira, Structuring effects of chemicals from the sea fan *Phyllogorgia dilatata* on benthic communities. *PeerJ* **5**, e3186 (2017).
65. M. Maldonado, Sponge waste that fuels marine oligotrophic food webs: A re-assessment of its origin and nature. *Mar. Ecol.* **37**, 477–491 (2016).
66. J. E. Thompson, K. D. Barrow, D. J. Faulkner, Localization of two brominated metabolites, aerothionin and homoaerothionin, in spherulous cells of the marine sponge *Aplysina fistularis* (= *Verongia thiona*). *Acta Zool.* **64**, 199–210 (1983).
67. M. A. Barbour, D. J. Kliebenstein, J. Bascompte, A keystone gene underlies the persistence of an experimental food web. *Science* **376**, 70–73 (2022).
68. D. R. Beukes, M. T. Davies-Coleman, Novel polypropionates from the South African marine mollusc *Siphonaria capensis*. *Tetrahedron* **55**, 4051–4056 (1999).
69. M. E. Frisch, G. W. Trucks, H. B. Schlegel, G. E. Scuseria, M. A. Robb, J. R. Cheeseman, G. Scalmani, V. P. Barone, G. A. Petersson, H. J. Nakatsuji, X. Li, M. Caricato, A. V. Marenich, J. Bloino, B. G. Janesko, R. Gomperts, B. Mennucci, H. P. Hratchian, J. V. Ortiz, A. F. Izmaylov, J. L. Sonnenberg, D. Williams-Young, F. Ding, F. Lipparini, F. Egidi, J. Goings, B. Peng, A. Petrone, T. Henderson, D. Ranasinghe, V. G. Zakrzewski, J. Gao, N. Rega, G. Zheng, W. Liang, M. Hada, M. Ehara, K. Toyota, R. Fukuda, J. Hasegawa, M. Ishida, T. Nakajima, Y. Honda, O. Kitao, H. Nakai, T. Vreven, K. Throssell, J. A. Montgomery, Jr., J. E. Peralta, F. Ogliaro, M. J. Bearpark, J. J. Heyd, E. N. Brothers, K. N. Kudin, V. N. Staroverov, T. A. Keith, R. Kobayashi, J. Normand, K. Raghavachari, A. P. Rendell, J. C. Burant, S. S. Iyengar, J. Tomasi, M. Cossi, J. M. Millam, M. Klene, C. Adamo, R. Cammi, J. W. Ochterski, R. L. Martin, K. Morokuma, O. Farkas, J. B. Foresman, D. J. Fox, *Gaussian 16, Revision B.01*, (Gaussian Inc., 2016).
70. A. Prjibelski, D. Antipov, D. Meleshko, A. Lapidus, A. Korobeynikov, Using SPAdes de novo assembler. *Curr. Protoc. Bioinformatics* **70**, e102 (2020).
71. L. T. Nguyen, H. A. Schmidt, A. von Haeseler, B. Q. Minh, IQ-TREE: A fast and effective stochastic algorithm for estimating maximum-likelihood phylogenies. *Mol. Biol. Evol.* **32**, 268–274 (2015).
72. R. Patro, G. Duggal, M. Love, R. Irizarry, C. Kingsford, Salmon provides fast and bias-aware quantification of transcript expression. *Nat. Methods* **14**, 417–419 (2017).
73. J. H. Zar, *Biostatistical Analysis*, 2nd ed., (Prentice-Hall, 1984).
74. N. McLain, L. Camargo, C. R. Whitcraft, J. G. Dillon, Metrics for evaluating inundation impacts on the decomposer communities in a southern California coastal salt marsh. *Wetlands* **40**, 2443–2459 (2020).
75. EPA, Ecological Processes: What are the trends in the ecological processes that sustain the nation's ecological systems? (United States Environmental Protection Agency, 2020). https://epa.gov/report-environment/ecological-processes.
76. P. J. Somerfield, R. M. Warwick, Meiofauna techniques in *Methods for the Study of Marine Benthos* A. Eleftheriou (ed), (John Wiley & Sons, 2013).
77. J. T. Carlton, *The Light and Smith Manual: Intertidal Invertebrates from Central California to Oregon* (The Univ. of California, 2007).
78. D. Bates, M. Mächler, B. Bolker, S. Walker, Fitting linear mixed-effects models using lme4. *J. Stat. Softw.* **67**, 1–48 (2015).
79. R Core Team, R: A language and environment for statistical computing. (R Foundation for Statistical Computing, Vienna, Austria, 2023).

Acknowledgments: We gratefully acknowledge assistance from L. Harris, A. Lim, A. McCurdy, B. Pernet, and C. Whitcraft. For access to field sites, we thank L. Arkinstall, T. Leland, J. Passarelli, and B. Spies. **Funding:** This work received funding from the U.S. National Science Foundation grant IOS-2127110 (E.M.W. and P.J.K.), U.S. National Science Foundation grant OCE-0648606 (P.J.K.), U.S. National Science Foundation grant IOS-2127111 (E.W.S.), U.S. National Science Foundation grant IOS-2127112 (A.J.Z.), U.S. National Science Foundation grant PRFB-1907177

(S.A.C.), U.S. National Institutes of Health Intramural Program award NIDDK DK031135 (C.A.B.), and CSU Council on Ocean Affairs, Science & Technology (COAST) Graduate Student Research Award (P.W.). **Author contributions:** Conceptualization: P.W., E.W.S., and P.J.K. Funding acquisition: S.A.C., C.A.B., A.J.Z., E.M.W., E.W.S., and P.J.K. Data curation: P.S., M.G., and P.J.K. Investigation: P.S., P.W., H.N., A.P.R., M.G., S.I.O., E.P., and P.J.K. Formal analysis: P.S., P.W., H.N., A.P.R., M.G., S.I.O., E.M.W., C.A.B., L.B., A.J.Z., E.W.S., and P.J.K. Resources: S.A.C. Supervision: E.W.S. and P.J.K. Visualization: P.S. and P.J.K. Writing—original draft: P.J.K. Writing—review and editing: all authors. **Competing interests:** The authors declare that they have no competing interests.

Data and materials availability: Sequences for AFPK enzymes are available from the NCBI repository (AmPKS 1, OR565848; AmPKS 2, OR565849). All data needed to evaluate the conclusions in the paper are present in the paper and/or the Supplementary Materials.

Submitted 16 April 2024
Accepted 24 September 2024
Published 30 October 2024
10.1126/sciadv.adp8643